Isotropic Bipolaron-Fermion-Exchange Theory and Unconventional Pairing in Cuprate Superconductors

J. -B. Bru*
IKERBASQUE, Basque Foundation for Science, 48011, Bilbao, Spain

W. de Siqueira Pedra† and A. Delgado de Pasquale‡
Instituto de Física, Universidade de São Paulo. Rua do Matão, 187 CEP 05508-090, São Paulo, Brazil
(Dated:)

The discovery of high-temperature superconductors in 1986 represented a major experimental breakthrough (Nobel Prize 1987), but their theoretical explanation is still a subject of much debate. These materials have many exotic properties, such as d- and p-wave pairing and density waves. The appearance of unconventional pairing is examined from a microscopic model, taking into account important properties of hole-doped copper oxides. We consider an exchange interaction between fermions and dominantly inter-site bipolarons to be the mechanism which leads to the pairing. We connect its momentum dependency to the well-established fermion-phonon anomalies in cuprate superconductors. Since charge carriers in these materials are strongly correlated, we add a screened Coulomb repulsion to this exchange term. We avoid any ad hoc assumptions like anisotropy, but rather provide a microscopic explanation of unconventional pairing for coupling strengths that are in accordance with experimental facts. One important outcome is a mathematically rigorous elucidation of the role of Coulomb repulsion in unconventional pairing, which is shown to be concomitant with a strong depletion of superconducting pairs. Our theory, applied to the special case of LaSr 214, predicts at optimal doping (i) a coherence length of 21Å, which is the same as that obtained from the Ginzburg–Landau critical magnetic field measured for this material, and (ii) d-wave pair formation in the pseudogap regime, i.e., at temperatures much higher than the superconducting transition temperature. The understanding of pairing symmetry and the pseudogap phase are central issues in the theoretical comprehension of high-temperature superconductivity, with possible technological applications like s-, d-, and p-wave Josephson junctions used nowadays in quantum computers.

Keywords: High Tc-Superconductivity, phonon anomaly, cuprates, bipolaron, d-wave, s-wave, p-wave, pseudogap.

INTRODUCTION

In all cuprates, there is undeniable experimental evidence of strong on-site Coulomb repulsions, leading to the universally observed Mott transition at zero doping [1, 2]. This phase is characterized by a periodic distribution of fermions (electrons or holes) with exactly one particle per lattice site. Doping copper oxides with holes or electrons can prevent this situation. Instead, at sufficiently small temperatures a superconducting phase is achieved, as first discovered in 1986 for the copper oxide perovskite $La_{2-x}Ba_xCuO_4$ [3].

As explained in [4–6], charge transport only occurs in cuprates within two-dimensional isotropic CuO_2 layers made of Cu^{++} and O^{--} ions. The lattice composed by copper and oxygen ions in these layers is cubic and thus invariant under the group $\{0, \pi/2, \pi, 3\pi/2\}$ of rotations (C_4 symmetry). Wave functions on the lattice can be uniquely decomposed into three orthogonal components, each having a well-defined parity with respect to the lattice rotations: The s-wave component is invariant under these 4 rotations, the d-wave one is antisymmetric with respect to the $\pi/2$-rotation and the p-wave one is antisymmetric with respect to the π-rotation (reflection over the origin), just like "s", "d" and "p" atomic orbitals.

In conventional superconductivity, like in metallic superconductors, charge carriers are electron pairs with zero total spin and s-wave symmetry, i.e., their wave function is invariant under any lattice rotation. The situation for superconducting cuprates is, however, more complex. On the one hand, it is believed that spin-triplet and spin-singlet states are pairs with, respectively, odd and even parity with respect to the π-rotation. On the other hand, it is firmly established that fermion pairs in cuprate superconductors have zero total spin [7]. This leads to s- or d-wave superconductivity. Since the s-wave pairing is supposed to be suppressed by the strong on-site Coulomb repulsion, d-wave superconductivity is expected. This prediction is experimentally confirmed. See [2, 5, 7].

Nevertheless, as explained in [8, 9], 100% of d-wave pairing is only demonstrated for surface sensitive experiments like those in [7], such as tunnelling and photoemission. For experiments involving bulk properties, a non-vanishing small s-wave component is experimentally seen [9–16]. This means, in particular, that the s-wave component of the wave function depends on the distance from the surface [11]. Müller [8] emphasizes that this is a consequence of the symmetry breaking present at the superconducting/vacuum interface, together with the

smallness (a few nanometers) of the coherence length ξ in cuprate superconductors. Therefore, a theoretical explanation of unconventional pairing (as a function of material features) including the delicate interplay between s- and d-wave superconductivity may pave the way to a microscopic theory of high-temperature superconductivity. In this paper we tackle this issue via controlled solutions of a model that takes into account strong, screened Coulomb repulsions.

Some of the more popular theoretical models for cuprate superconductors are summarized in [5, Chap. 7]. They are usually inspired by the celebrated Hubbard model in two dimensions. Explicit solutions of this model are, unfortunately, only available in one dimension and its use for higher dimensions necessarily requires either numerical methods or the derivation of more tractable effective models, for example via perturbative arguments. In this context, one can use either the strong or weak coupling regime, but both cases are unrealistic with respect to physical properties of cuprates: The strong coupling regime yields to a ferromagnetic phase only [17, 18], while any weak coupling approach is not compatible with the experimentally observed, strong, on-site Coulomb repulsion in CuO_2 layers.

In connection to the Hubbard model are the t-J model (an extension of the Heisenberg Hamiltonian adapted to weakly hole-doped cuprates), the resonating valence bond (RVB) theory in the underdoped regime, and the effective spin fluctuation model. These theories have successfully predicted a d-wave superconducting ground state, but the critical temperature deduced from the famous t-J or RVB theories of superconductivity seems to be very small, if it exists at all [8]. Moreover, [19] claims that a magnetic pairing mechanism based on the spin-fermion model and on the t-J model cannot explain tunneling, ARPES, or neutron data in cuprate superconductors.

As stressed in [20, Part VII], an important phenomenon which is usually *not* taken into account in these theoretical studies is the existence of polaronic quasiparticles in relation with the very strong Jahn-Teller (JT) effect associated with copper ions. Indeed, at least as early as 1990, the existence of JT bipolarons in copper oxides is discussed in the literature [21]. The role of polarons is also emphasized in the celebrated paper [3] since it was the JT effect that led to the discovery of superconductivity in cuprates. See [8, p. 2] or [9, 22].

Nevertheless, in the recent review [2] on high-temperature superconductivity the word "polaron" does not even appear. Indeed, some scientific communities focus instead on the antiferromagnetic properties of copper oxides. It is intriguing, however, that the *ferromagnetic* strontium ruthenate Sr_2RuO_4 can support superconductivity within RuO_2 layers [23, 24]. This phenomenon appears at much lower temperature than in cuprates, making the copper and maybe the antiferromagnetism important, but not necessarily pivotal, to achieve superconductivity.

On the other hand, several many-polarons theories of superconductivity exist, as explained in [5, Section 7.4.3]. These theories are also based on Hubbard or t-J models with Fröhlich electron-phonon interactions. For instance, the bipolaron theory of Alexandrov and coauthors is based on *light* bipolarons [25] as charge carriers. Alexandrov claims in [26, p. 4] that "cuprate bipolarons are relatively light because they are intersite rather than on-site pairs due to the strong on-site repulsion, and because mainly c-axis polarized optical phonons are responsible for the in-plane mass renormalization." See for instance [26–29] and references therein.

In [30] a theory based on the t-J model with two (spin and charge) fermionic channels connected via Fröhlich electron-phonon interactions is numerically studied. This theory seems to be promising since it gives realistic critical temperatures, in contrast to the single-band t-J model, and reproduces both the doping dependence of the pseudogap temperature and the giant oxygen isotope effect, as explained in [8, Section 3].

However, even after three decades of theoretical studies, including the metaphoric string theory approach to condensed matter via the AdS/CFT duality, and in spite of many significant advances, there is still no widely accepted explanation of the (polaronic or not) microscopic origin of unconventional superconductivity. A large amount of numerical and experimental data is available, but no particular pairing mechanism (through, for instance, antiferromagnetic spin fluctuations, phonons, etc.) has been firmly established [5, Section 7.6]. In fact, the debate seems to be strongly polarized [31] between those using a purely electronic/magnetic microscopic mechanism and those using electron-phonon mechanisms.

Our theoretical approach differs from all theories mentioned above and predicts, for cuprates, dominant d-wave pair formation in the *pseudogap* regime, that is, at temperatures much higher than the superconducting transition temperature (see, e.g., [32]). It stems from a microscopic model – first proposed in 1985 by Ranninger-Robaszkiewicz [33] (see also [34, 35] or [5, Section 7.4.3]) and independently by Ionov [36] – which has *never* been investigated in the presence of *strong* Coulomb repulsions.

EXPERIMENTAL FOUNDATIONS OF OUR MICROSCOPIC APPROACH

Bipolaron-fermion-exchange Interaction

In contrast to [25, 26] we assume that Jahn-Teller (JT) bipolarons in cuprates are *not* the main charge carriers in the superconducting phase. Polarons and thus bipolarons (more generally, n-polarons, $n \in \mathbb{N}$) are rather charge carriers that are self-trapped inside a strong and local lattice deformation that surrounds

them. They are formed from fermions "dressed with phonons". A priori, such (strong and local) lattice deformations attached to n-polarons can barely move and this is not in accordance with the known mobility of superconducting charge carriers. In fact, like JT polarons [37], JT bipolarons in copper oxides probably have a large mass, even in the case of inter-site bipolarons. Note that a very large mass has indeed been demonstrated in [38] from experiments, but this result has been criticized in [39]. We show that the existence of light, bound pairs in oxygen layers is not in contradiction with (mediating) heavy bipolarons in copper layers.

Our assumption is supported by the fact that both fermionic and polaronic quasiparticles have been experimentally observed within cuprates via magnetic susceptibility, EXAFS, pulse-probe, photoexcitation, NMR/NQR, etc. See [8, 40] and references therein. Moreover, by using the velocity of sound in copper oxides to express the lifetime of bipolarons in terms of a length ℓ, as estimated from [41], one sees a lifetime comparable to the lattice spacing. In fact, near the critical temperature, remarkably $\ell \simeq \xi$, the coherence length in cuprate superconductors. This suggests a strong exchange interaction between the bipolaronic state and fermion pairs. Representing the two-dimensional CuO_2 layer by $\mathbb{Z}^2$ in lattice units, we therefore use a coupling function v, invariant under the $\pi/2$-rotation, to define a bipolaron-fermion (exchange) interaction

$$\varkappa v(x-y)(b_x^\dagger c_y + c_y^\dagger b_x), \quad x, y \in \mathbb{Z}^2, \tag{1}$$

where the bosonic operator b_x annihilates a bipolaron at lattice position $x \in \mathbb{Z}^2$, whereas c_x annihilates a fermion pair around $x \in \mathbb{Z}^2$. See Eq. (3). The parameter $\varkappa \geq 0$ is the bipolaron-fermion exchange strength. See Eq. (2). The space structure of the bipolaron is implemented in the definition of c_x. See Eq. (4). Note that the interpretation of mediating bosons as being bipolarons is natural for copper oxides (see discussions below), but one may also see b_x as the annihilation of another type of boson like, for instance, an exciton (spin waves, density waves, etc.).

Observe that mobile holes added to CuO_2 layers are found in the oxygen band, where superconductivity is experimentally demonstrated to take place. In particular, holes in the copper band cannot alone produce superconductivity, see for instance [4, p. 133]. The (JT) bipolaron-fermion-exchange interaction takes into account this observation since (superconducting) fermion pairs are only in the oxygen band, while bipolarons also involve the copper band, by being formed in the oxygen ligands of copper ions via the strong JT effect associated with Cu. As stressed in [8, Sect. 5.2], these JT bipolarons should have zero total spin because of the *antiferromagnetic* character of copper-oxides. Indeed, strong antiferromagnetic copper spin correlations in CuO_2 layers are ubiquitous in cuprates [5, Chap. 3]. Even if static antiferromagnetism is rapidly suppressed by doping, resonant inelastic X-ray scattering in the superconducting phase, for $La_{2-x}Sr_xCuO_4$ (LaSr 214) [42] and other copper-oxide compounds [43] like underdoped $YBa_2Cu_4O_8$ and overdoped $YBa_2Cu_3O_7$, reveals a persistence of strong antiferromagnetic correlations, similar to those in the isolating phase. In this context, the formation of a JT *polaron* strongly disturbs [71] the antiferromagnetic order within the CuO_2 layers. Spinless, strongly localized inter-site bipolarons do not have this property, i.e., they do not modify the antiferromagnetic background when they are created. In other words, the antiferromagnetic character of cuprates make the creation of spinless JT bipolarons much more favorable than other polaronic configurations. A similar issue is discussed in [8, Sect. 4] to justify the poor mobility of polarons.

The interaction (1) is reminiscent of the celebrated microscopic theory of superfluid Helium 4 via the non-diagonal part of the Weakly Imperfect Bogoliubov Hamiltonian, known to imply a *depletion* of the Bose condensate [44, 45]. It is *completely different* from the Fröhlich electron-phonon interaction leading to the BCS theory of conventional superconductivity. It corresponds to what was first proposed in [33, 36], except that we use *inter-site* instead of on-site bipolarons, similar to [46].

The existence of inter-site bipolarons was proposed by Mihailovic and Kabanov [47, 48], based on facts like those derived from inelastic neutron scattering experiments [49]. In our microscopic approach it turns out that the inter-site character of bipolarons is essential to get d-wave pairing. Indeed, we aim to rigorously derive this property (among other phenomena typical to cuprate superconductors) from strictly isotropic models with strong on-site Coulomb repulsions, in contrast to [46] which neglects the Coulomb repulsion and postulates that the mediating boson is formed out of (ad hoc) two d-wave paired electrons.

A first mathematical result in this direction has been obtained in [50] for an isotropic model including a bipolaron-fermion (exchange) interaction and the on-site Coulomb repulsion. In this model, we analytically show the existence of a *pure* d-wave pairing, in the strong coupling limit. By contrast, in the present study we fix the parameters according to experimental data, and the definition used for the fermion pair annihilation operator c_x captures the physics of JT bipolarons in copper oxides in a more realistic way than in [50]. We then study the model by *rigorous* semi-analytical methods, meaning that they are partially numerical, but always rigorously controlled. Indeed, we obtain the minimum energy wave functions for a two-fermion-one-bipolaron system in terms of solutions of a continuum of *non-linear* finite-dimensional equations. Exactly as was done in [50], these equations are derived from the Birman-Schwinger principle applied to the fiber (constant total quasimomentum) Hamiltonians of the total (translation invariant) three-particles Hamiltonian. These non-linear, but explicit, equations are then studied numerically, as they are defined in small dimensions. Once the numerical solutions of the fermionic part of the wave function are

established, we study their symmetry under the $\pi/2$- and π-rotations. In particular, we analyze the s-, d- and p-wave symmetry for the fermion pair, unlike in [50] where p-wave pairing is not considered.

Exchange Coupling Function and Electron-phonon Anomalies

In contrast to [46] the exchange interaction (1) is isotropic and the momentum dependency of the Fourier transform of the coupling function v is pivotal in our microscopic approach. Its choice is based on experimental facts [51, 52] associated with *electron-phonon anomalies* in cuprate superconductors.

Phonon anomalies can be experimentally detected in doped cuprates via (i) the softening of phonon dispersion and (ii) the broadening of phonon lines:

(i) By softening of phonon dispersion, we mean a decrease of the phonon energy at a fixed wavelength in the presence of doping. In doped La_2CuO_4, the effect is maximized in the $(1,0,0)$ or $(0,1,0)$ (antinodal) directions at half-breathing bond-stretching mode, that is to say the quasimomenta $(\pi,0)$ and $(0,\pi)$ in the normalized Brillouin zone $\mathbb{T}^2 \doteq [-\pi,\pi)^2$ of two-dimensional CuO_2 layers (reciprocal lattice units). See [53, 54]. By [54, Figs. 2, 7], the growth rate of the softening for $(\pi,0)$ and $(0,\pi)$ is almost constant up to optimal doping and is considerably smaller afterwards. As explained in [49], the softening of phonon dispersion seems to be ubiquitous as it is observed for other superconductors like $YBa_2Cu_3O_{6+y}$ and the (non-cuprate) $Ba_{1-x}K_xBiO_3$.

(ii) By broadening of phonon lines, we mean an increase in the full-width half maximum (FWHM) of the phonon frequency distribution at a fixed wavelength in the presence of doping. In doped La_2CuO_4, the phenomenon is strongest for quasimomenta $(\pm\pi/2,0)$ and $(0,\pm\pi/2)$ in CuO_2 layers and around the (optimal) doping point for which the critical temperature of superconductivity is the highest, by [54, Fig. 2] and [55]. See also [51], which additionally reviews similar results on other copper oxides.

Both cases (i) and (ii) indicate a singular electron-phonon interaction at quasimomenta $(\pm\pi/2,0)$, $(0,\pm\pi/2)$, $(\pi,0)$ and $(0,\pi)$. As illustrated by [56, Fig. 1 (a)], the dispersion relation at $(\pm\pi/2,0)$ and $(0,\pm\pi/2)$ is well-reproduced, even at optimal doping, using the Density Functional Theory (DFT). By contrast, the dispersion relation at $(\pi,0)$ and $(0,\pi)$ is *not* well-reproduced by the same theory. In the overdoped La_2CuO_4, for which no superconducting phase appears, the dispersion relation at *all* quasimomenta in the antinodal direction is well-reproduced by the DFT [51, Fig. 18 (b)]. Since the DFT used in [56, Fig. 1 (a)] does not take into account the formation of compound particles out of phonons and fermions, this suggests

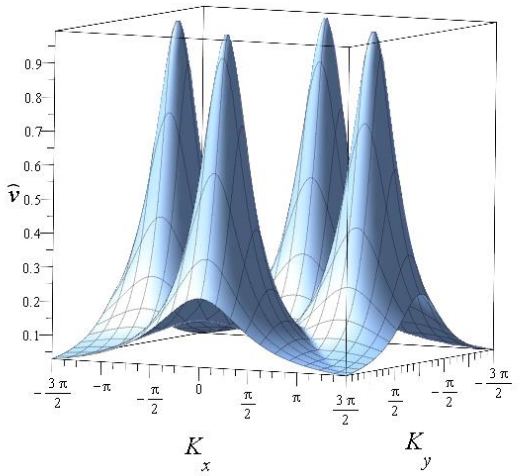

Figure 1: Exchange coupling function $\hat{v}$ for $K \in [-3\pi/2, -3\pi/2]^2 \supset \mathbb{T}$.

the existence of additional quasiparticles that strongly interact with electrons and phonons at quasimomenta $(\pi,0)$ and $(0,\pi)$ and at moderate doping. In our theory they are interpreted as being JT bipolarons. In contrast, the congruence between DFT and experimental data for phonon dispersions at $(\pm\pi/2,0)$ and $(0,\pm\pi/2)$ makes the formation of such particles unlikely in this region of the Brillouin zone.

The electron-phonon anomalies (i) at quasimomenta $(\pi,0)$ and $(0,\pi)$ are possibly related to Fermi surface nesting [57] and van Hove singularities in CuO_2 planes, that is, peaks in the electronic density of states coming from saddlelike regions of the dispersion relation of fermions (electrons or holes). Their connection with (d-wave) superconductivity in copper oxides has been discussed in, e.g., [7, Sect.VI] and references therein. This relationship is mathematically confirmed in our model; see **(b)** in the next section. Moreover, ARPES experiments demonstrate that, even for temperatures well above the superconducting transition temperature, a so-called pseudogap appears at quasimomenta $(\pi,0)$ and $(0,\pi)$ in the normalized Brillouin zone. This corresponds with the pseudogap regime found in all cuprates. See [2, Fig. 4] and references therein.

To account for the aforementioned observations, we fix a coupling function v that is isotropic, i.e., invariant with respect to the $\pi/2$-rotation, and with Fourier transform $\hat{v}$ taking maximum values at half-breathing bond-stretching modes, that is, $(\pi,0)$ and $(0,\pi)$ in the normalized Brillouin zone $\mathbb{T}^2 \doteq [-\pi,\pi)^2$, as sketched in Fig. 1.

The focus on the phonon anomalies (i) can, however, be subject to debate. In fact, since they subsist on overdoped La_2CuO_4 for which there is no longer any superconducting phase, [51, 54] claim that (i) may be more

"related to the increase of the metallicity with doping rather than to the mechanism of superconductivity". In the current study we do not consider the superconducting phase, which is a *collective* phenomenon, but only the pseudogap regime which is expected to be related to the formation of fermion pairs. The doping that yields the highest pseudogap temperature is near zero doping. Indeed, the peudogap temperature decreases monotonically as a function of doping: It is approximately $750K$ at $x \simeq 0$, $400K$ at $x = 0.15$ (optimal doping for superconductivity), and $200K$ at $x = 0.2$ [32, Fig. 26]. Therefore, a maximal phonon anomaly at optimal doping $x = 0.15$ cannot be directly used to decide at which point of the Brillouin zone the bipolaron-fermion exchange is the strongest. Indeed, the strength of anomalies (i)-(ii) depends on the density of charged carriers, and not only on the strength of the fermion-phonon interaction. In particular, the monotonic increase of the phonon anomalies (i) until overdoped regimes might simply reflect the increase of the fermion density. Moreover, in the physical picture proposed here for fermion pairing, the binding energy of bipolarons imposes an upper bound on the temperature at which pair formation is possible. Similar to the behavior of the pseudogap temperature, [58] shows a clear decrease of the binding energy of bipolarons as a function of doping x for $La_{2-x}Sr_xCuO_4$. For instance, it is near $1500K$ at $x \simeq 0$, $500K$ at $x = 0.15$ (optimal doping), and $200K$ at $x = 0.2$ [58, Fig. 2]. Additionally, one would expect that the pseudogap temperature is related to the binding energy of (bipolaron-dressed) fermion pairs. In our model, this energy turns out to be approximately proportional to the bipolaron-fermion exchange strength $\varkappa \geq 0$ (cf. (1) and Fig. 6). This indicates that this effective coupling decreases monotonically as a function of doping, which is coherent with the behavior of the binding energy of bipolarons as a function of doping and with the accuracy of DFT at large doping.

Finally, concerning the superconducting transition temperature, we also observe the following: The bipolaron-fermion (exchange) interaction should produce an effective attractive coupling γ for fermions, as in the BCS-Fröhlich theory. Mathematically rigorous results [59, 60] suggest that, at constant γ, the critical temperature of the superconducting phase rapidly decreases as a function of doping after reaching the optimal fermion density. In fact, [60, Fig. 16] predicts the appearance of a mixed (superconducting) phase for hole-overdoped cuprates. This seems to be compatible with the superfluid density observed in doped La_2CuO_4 [61, Fig. 2(b,c) & 3(b)], which is essentially linear as a function of temperature. This phenomenon appears because a strong Coulomb repulsion causes a discontinuous superfluid density as a function of chemical potential [59, 60]. Meanwhile, an interaction like (1) together with repulsion terms tends to produce the same behavior. For instance, the Weakly Imperfect Bogoliubov Hamiltonian manifests the same property when Bose condensation appears [44, Fig. 10].

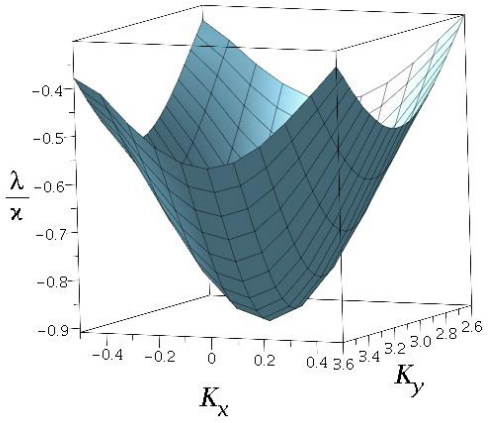

Figure 2: Binding energy λ (in units of $\varkappa$) as a function of the total quasimomentum K for prototypical parameters.

Phenomenological Consequences for LaSr 214

The following results correspond to the two-fermion-one-bipolaron sector at prototypical parameters taken from experiments on La_2CuO_4 (LaSr 214) near optimal doping:

(a) In the ground state, we demonstrate the existence of bound fermion pairs with total quasimomentum near either $(\pi, 0)$ or $(0, \pi)$, see Fig. 2. The pairs have a large bipolaronic component, i.e., they are *dressed* bound fermion pairs, see Fig. 3. Again by Fig. 2, the dressed fermion pairs behave like massive particles which have minimum energy and are at rest whenever their quasimomentum equals $(\pi, 0)$ or $(0, \pi)$.

(b) The p-wave component of dressed bound fermion pairs with quasimomentum $(\pi, 0)$ or $(0, \pi)$ is always vanishing (Corollary 1.1). I.e., the C_2 symmetry is *not* broken in this case, like for $YBa_2Cu_3O_{6+\delta}$ [62]. By contrast, if the Fourier transform $\hat{v}$ of the coupling function v is concentrated near $(\pm\pi/2, 0)$ and $(0, \pm\pi/2)$, then the p-wave component of pairs at rest dominates. See below Fig. 16. As p-wave pairing has never been found in cuprate superconductors, this fact strengthens our assumption of a function $\hat{v}$ taking its local maxima only at $(\pi, 0)$ and $(0, \pi)$.

(c) By Fig. 4, we obtain 83.5% d-wave pairing and 16.5% s-wave pairing, in accordance with what was crudely deduced from experimental data [13–15]. See also [8, Section 6]. The existence of dominant d-wave pairing and a very strong depletion [72] (ca. 90%), as observed in [61], are concomitant. See dot-dashed lines in Figs.

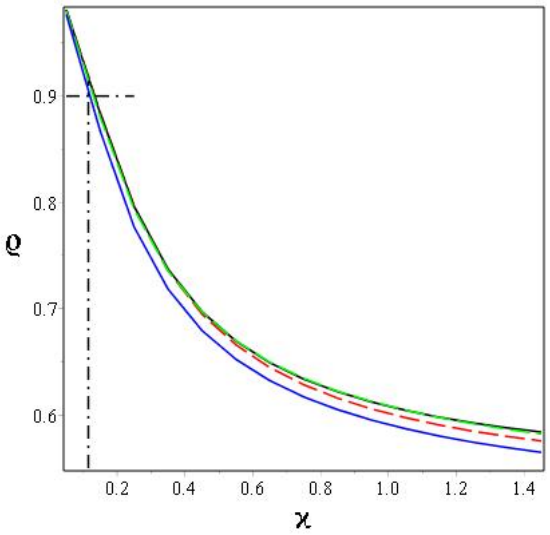

Figure 3: Depletion ϱ as a function of $\varkappa$ at total quasimomentum $K = (0, \pi)$ for on-site repulsion strengths $U_0 = 1.461$ (blue), 5 (green), 15 (black), 50 (red). The vertical and horizontal dot-dashed lines highlight the 90% depletion for the prototypical parameters.

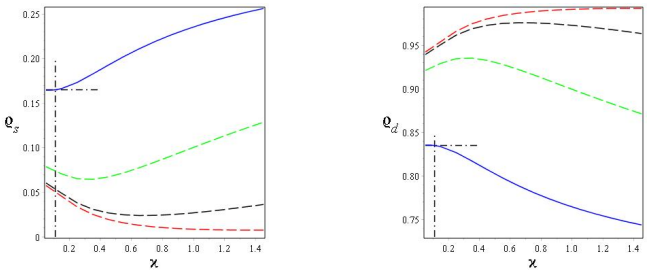

Figure 4: s- and d-wave densities (left and right, respectively) as functions of $\varkappa$ at total quasimomentum $K = (0, \pi)$ for on-site repulsion strengths $U_0 = 1.461$ (blue), 5 (green), 15 (black), 50 (red). The vertical dot-dashed lines highlight the prototypical parameter $\varkappa = 0.11eV$.

3 and 4. In particular, the C_4 symmetry is broken, as observed for $YBa_2Cu_3O_{6+\delta}$ [62].

(d) We compute at optimal doping a coherence length $\xi \simeq 8\mathbf{a} \simeq 21$Å ($\mathbf{a}$ is the lattice spacing), which is the same one obtained from the Ginzburg–Landau theory for this material. See Fig. 5 (in lattice units) and [6, Table 9.1]. Note that the understanding of the smallness of the size of Cooper pairs in cuprate superconductors is an important issue in the microscopic theory of high-temperature superconductivity.

(e) Our theory predicts that d-wave pairs dominate in the pseudogap regime, i.e., at temperatures much higher than the superconducting transition temperature of $39K$ for optimally-doped La_2CuO_4 [6, Fig. 5.1]. See black dot-dashed lines of Fig. 6. The pseudogap temperature is predicted to depend on the strength of the inter-site (Fig. 12), but not much on the on-site

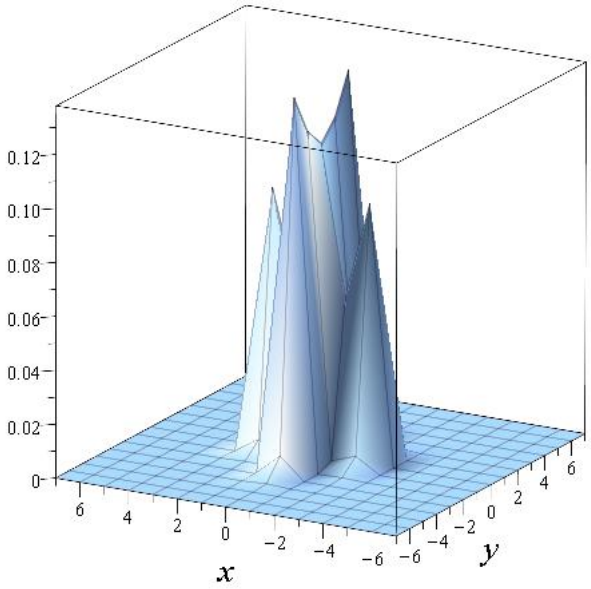

Figure 5: Normalized density $|\check{\psi}_{(0,\pi)}|^2$ of the dressed bound fermion pair as a function of the (relative) position space at total quasimomentum $K = (0, \pi)$ for the prototypical parameters.

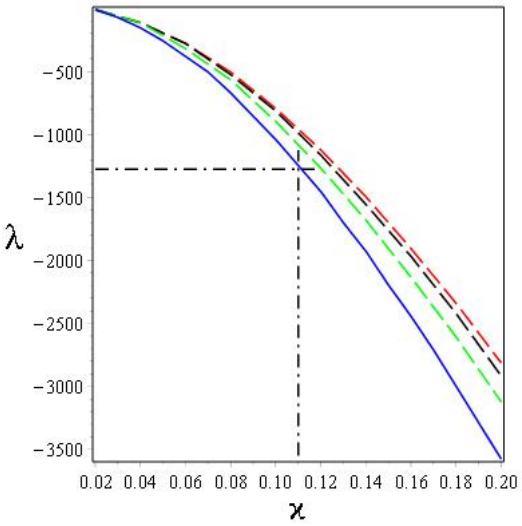

Figure 6: Binding energy λ (in Kelvin) as a function of $\varkappa$ at total quasimomentum $K = (0, \pi)$ for on-site repulsion strengths $U_0 = 1.461$ (blue), 5 (green), 15 (black), 50 (red). The vertical and horizontal dot-dashed lines highlight the prototypical parameter $\varkappa = 0.11eV$.

(Fig. 6), repulsion. However, at prototypical parameters, a stronger screening of the Coulomb interaction would not significantly enhance the pseudogap temperature (cf. Fig. 12). For optimally-doped La_2CuO_4, the pseudogap temperature is $400K$ [32, Fig. 26].

(f) On-site bipolarons imply an almost purely s-wave

pairing. A considerable suppression of the d-wave component of dressed bound fermion pairs is also found in the absence of Coulomb repulsions. See Fig. 13 (right) for more details. Consequently, both the electronic repulsion and the inter-site bipolarons are necessary to support a dominant d-wave pairing.

(g) Strong Coulomb repulsions are not necessary to get the strong (fermion) depletion measured in [61]. See Fig. 13 (left). The strong depletion is related, rather, to the large mass of bipolarons, as we see from Fig. 10. Moreover, the large pseudogap temperature [32, Fig. 26] is not compatible with light bipolarons. See Fig. 11. The very large mass of bipolarons estimated in [38] is nevertheless unnecessary for our microscopic theory to work: a bipolaron 10 times lighter would yield the same phenomenology, although it still has to be significantly heavier than the holes.

(h) The mass computed in [39] for charge carriers should be seen as an estimated mass for dressed bound fermion pairs instead of bipolarons. Our model predicts that a large effective mass m^{***} of dressed bound fermion pairs is not compatible with a depletion near 90% measured in [61]. More precisely, at such depletions, our microscopic theory implies that $m^{***} \leq 80 m_e$, where m_e is the electron mass. In fact, the precise value of m^{***} depends strongly on the coupling function $\hat{v}$ near its maximum (at van Hove points in this case). Using the estimate $m^{***} \in [m_e, 3m_e]$ of [39], we conclude that $\hat{v}$ is only *weakly* concentrated around half-breathing bond-stretching mode, see Fig. 1. This is coherent with the softening of phonon dispersion displayed in [54, Fig. 2].

(i) Finally, the hard-core regime, i.e., $U_0 \gg 1$, captures the physical properties of dressed bound fermion pairs quite well. See Figs. 3 (depletion), 4 (s- and d-wave components), and 6 (binding energy). The space structure of pair correlations is also well-described in this regime: As compared to Fig. 5, only the density at the origin is affected, in that it is strongly suppressed, which is in accordance with the larger d-wave component seen in Fig. 4, for $U_0 \gg 1$. By contrast, neither the small hopping nor the large (simultaneously on-site and inter-site) repulsion regimes can correctly reproduce the phenomenology of dressed bound fermion pairs at prototypical parameters for doped La_2CuO_4. See Figs. 12, 14 and 15. This demonstrates that pairing in cuprates is a highly quantum mechanical phenomenon.

BIPOLARON-FERMION MICROSCOPIC MODEL

We denote by $\mathcal{F}_\pm$ the bipolaron (bosonic, $+$) and fermionic ($-$) Fock spaces with one-particle Hilbert space $\ell^2(\mathbb{Z}^2;\mathbb{C})$. The Hilbert space associated with the compound system is $\mathcal{F}_- \otimes \mathcal{F}_+$. Creation and annihilation operators at $x \in \mathbb{Z}^2$ (lattice units) are respectively denoted by $b_x^\dagger$, b_x for bipolarons and $a_{x,s}^\dagger$, $a_{x,s}$ for fermions (electrons or holes) with spin $s \in \{\uparrow, \downarrow\}$. See [50] for more details.

For any hopping amplitude $\epsilon \geq 0$, repulsions $U, U_0 \geq 0$, range $r \geq 0$ and exchange strength $\varkappa \geq 0$, we define the Hamiltonian

$$\mathbf{H} \doteq \epsilon \mathbf{T} + U_0 \mathbf{W}_{\mathrm{f-f}}^{(0)} + U \mathbf{W}_{\mathrm{f-f}}^{(r)} + \varkappa \mathbf{W}_{\mathrm{b-f}}, \qquad (2)$$

where $\mathbf{W}_{\mathrm{f-f}}^{(0)}$, $\mathbf{W}_{\mathrm{f-f}}^{(r)}$ are, respectively, the on-site and inter-site fermion-fermion repulsions, and $\mathbf{W}_{\mathrm{b-f}}$ is the bipolaron-fermion interaction, while the kinetic terms are

$$\mathbf{T} \doteq h_b \left(-\frac{1}{2} \sum_{x,y \in \mathbb{Z}^2, |x-y|=1} b_x^\dagger b_y + 2 \sum_{x \in \mathbb{Z}^2} b_x^\dagger b_x \right)$$
$$-\frac{1}{2} \sum_{s \in \{\uparrow,\downarrow\}, x,y \in \mathbb{Z}^2, |x-y|=1} a_{x,s}^\dagger a_{y,s} + 2 \sum_{s \in \{\uparrow,\downarrow\}, x \in \mathbb{Z}^2} a_{x,s}^\dagger a_{x,s}.$$

Here, $h_b \geq 0$ is the hopping amplitude of bipolarons relative to that of fermions.

For $r \geq 0$ and $\lambda > 0$, the screened Coulomb repulsion of fermions is defined by the density-density interactions

$$\mathbf{W}_{\mathrm{f-f}}^{(0)} \doteq \sum_{x \in \mathbb{Z}^2, s_1, s_2 \in \{\uparrow,\downarrow\}} a_{x,s_1}^\dagger a_{x,s_1} a_{x,s_2}^\dagger a_{x,s_2}.$$
$$\mathbf{W}_{\mathrm{f-f}}^{(r)} \doteq \sum_{\substack{x,z \in \mathbb{Z}^2, 1 \leq |z| \leq r \\ s_1, s_2 \in \{\uparrow,\downarrow\}}} \mathrm{e}^{-\lambda^{-1}|z|} a_{x,s_1}^\dagger a_{x,s_1} a_{x+z,s_2}^\dagger a_{x+z,s_2}.$$

The bipolaron-fermion (exchange) interaction term is defined by

$$\mathbf{W}_{\mathrm{b-f}} \doteq \sum_{x,y \in \mathbb{Z}^2} v(x-y)(b_x^\dagger c_y + c_y^\dagger b_x), \qquad (3)$$

with $v : \mathbb{Z}^2 \to \mathbb{R}$ being a $\mathbb{Z}^2$-summable function invariant under the $\pi/2$-rotation, and where

$$c_x \doteq \sum_{z \in \mathbb{Z}^2, |z| \leq 1} (a_{x+z,\uparrow} a_{x,\downarrow} + a_{x+z,\uparrow} a_{x-z,\downarrow}) \qquad (4)$$

is the annihilation operator of a fermion pair around $x \in \mathbb{Z}^2$. Compare (2) and (3)-(4) with (1).

The choice of the operator c_x is based on the structure of JT bipolarons obtained from *ab initio* calculations [63] for doped La_2CuO_4, as described in [8, Sect. 5.2]: JT bipolarons are formed by two antiparallel holes trapped in the oxygen ligands of two adjacent copper ions. Each oxygen ion lies between a unique pair of adjacent copper ions, as shown in Fig. 7. We can thus associate with each oxygen lattice site x an inter-site bipolaronic mode. We assume that the decay of such a bipolaron at x produces a pair of fermions (holes in this discussion) in the ligands of the corresponding copper ions. Additionally, the fermionic pair should lie between the copper ions and have its barycenter near x. These conditions are satisfied by the following spatial configurations of the fermion pair around $x \in \mathbb{Z}^2$: $(y_\uparrow, y_\downarrow) = (x, x+z)$ or $(x-z, x+z)$ with $|z| \leq 1$. Compare with (4) and see Fig. 7. Note

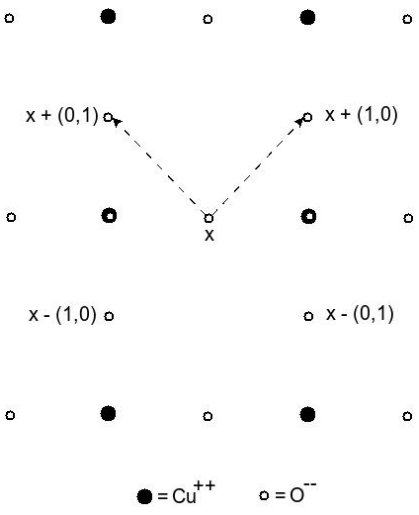

Figure 7: CuO_2 layer.

that we can easily assign different weights to each space configuration of fermion pairs.

Based on experimental facts, the microscopic structure of cuprate superconductors is isotropic. Hence, the real-valued function v on $\mathbb{Z}^2$ has to be invariant under the $\pi/2$-rotation so that the full Hamiltonian $\mathbf{H}$ *is invariant with respect to this rotation.* However, $\mathbf{W}_{\mathrm{b-f}}$, and thus $\mathbf{H}$, do *not* conserve the fermion number, in contrast to the Fröhlich electron-phonon interaction. A model similar to $\mathbf{H}$ for $r = 0$ is proposed in [50] to explain the appearance of d-wave paring at low energies in the presence of space isotropy.

Prototypical Parameters from Experiments

In theoretical studies using the Hubbard model, "standard" parameters are $\epsilon \simeq 1$, $U_0 \simeq 8$ (eV) and $U = 0$. In general, these are mainly derived by numerical methods. See, e.g., [5, Table 7.1.]. By contrast, in the current paper the choice of all parameters is based on experimental data for doped La_2CuO_4:

(ϵ) The hopping amplitude ϵ is obtained from the lattice spacing $\mathbf{a} = 2.672$Å [6, Sect. 6.3.1] of the oxygen ions [73] and the effective mass of mobile holes $m^* \simeq 4m_e$ [64, Fig. 2.] for $La_{2-x}Sr_xCuO_4$ with $x \in [0, 0.2]$, where m_e is the electron mass. This corresponds to $\epsilon = \hbar^2/\left(m^*\mathbf{a}^2\right) \simeq 0.266eV$. Compare with [5, Table 7.1.].

(U_0) The oxygen band is experimentally shown to be at the origin of superconductivity. The on-site repulsion strength U_0 is thus taken to be the first electron affinity of the oxygen ^{16}O, that is, the energy difference between $^{16}O^-$ (one hole in the oxygen anion $^{16}O^{--}$) and ^{16}O (two holes). By [65], $U_0 \simeq 1.461eV$. Note that $U_0\epsilon^{-1} \simeq 5.5$, which corresponds to the usual strong coupling regime of all previous theoretical studies (hard-core regime in the current paper).

(U) The inter-site repulsion results from the screening of the Coulomb repulsion. Therefore, we set $U = U_0$ as a prototypical parameter. The separation of the fermion-fermion repulsion into on-site and inter-site components is used to study the hard-core regime, which corresponds to large on-site repulsions.

(λ) [66] claims from experimental facts that the Thomas-Fermi screening length $\boldsymbol{\lambda}_{\mathrm{TF}}$ is comparable to the coherence length ξ in cuprate superconductors. For instance, $\boldsymbol{\lambda}_{\mathrm{TF}} \simeq 5$Å for $YBa_2Cu_3O_{7-\delta}$. For doped La_2CuO_4, we estimate this parameter, in two dimensions, via the well-known formula $\boldsymbol{\lambda}_{\mathrm{TF}} = (4\pi\boldsymbol{\varepsilon} \times \hbar^2)/\left(2m^*\mathbf{e}^2\right)$ (SI units) with $\mathbf{e}$ and $\boldsymbol{\varepsilon}$ being, respectively, the electronic charge and the dielectric constant of CuO_2 layers [67, Eqs. (1.21), (5.38) in Gaussian units]. By [68, Sect. VI.C], $\boldsymbol{\varepsilon} \simeq 30\boldsymbol{\varepsilon}_0$ where $\boldsymbol{\varepsilon}_0$ is the dielectric constant of the free space. This yields $\lambda = \boldsymbol{\lambda}_{\mathrm{TF}} \simeq 2$Å, similar to the $YBa_2Cu_3O_{7-\delta}$ case. (Note that some mathematically-rigorous results on the 2D screening of Coulomb interactions have been recently derived in [69, Theorem 3.2].)

(r) In two dimensions, the decay of the screened Coulomb repulsion is not exponential but rather polynomial [67, Eq. (5.41)]. In particular, even if $\boldsymbol{\lambda}_{\mathrm{TF}} \leq \mathbf{a}$, it is reasonable to consider the Coulomb repulsion for a few neighboring sites. We thus take the second screening parameter $r = 2$ as the default value.

(h_b) We deduce the relative hopping amplitude h_b from the effective mass of (partially pinned) bipolarons, as experimentally determined in [38]: $m^{**} \simeq 695m_e$. This corresponds to $h_b = m^*/m^{**} \simeq 0.00575$. Since [38] has been criticized for the bipolaronic mass being too large (see, e.g., [39]), we also consider larger values of the parameter h_b, up to 1.

$(\varkappa)$ The exchange coupling strength $\varkappa$ is chosen in order to get 90% depletion at $(\pi, 0)$ and $(0, \pi)$: A direct computation using [61, Fig. 2, Fig. 3(b)], with the lattice spacing $\mathbf{a}$ of the oxygen ions equal to 2.672Å, and the effective mass $m^* \simeq 4m_e$ [64, Fig. 2.] of mobile holes yields, for $La_{2-x}Sr_xCuO_4$ with $x \simeq 0.2$, a depletion of superfluid density approximately equal to 90%. By Fig. 3, $\varkappa \simeq 0.11eV$.

(v) As explained previously, we use a bipolaron-fermion coupling function v whose Fourier transform $\hat{v}$ is concentrated around $(\pi, 0)$ and $(0, \pi)$ in the Brillouin zone $\mathbb{T}^2 \doteq [-\pi, \pi)^2$. Similar to [47, 48], we choose $\hat{v}$ of the form

$$\left[\alpha\left((K_x - \pi)^2 + K_y^2\right) + 1\right]^{-1} \qquad \left(\text{resp.} \quad \left[\alpha\left(K_x^2 + (K_y - \pi)^2\right) + 1\right]^{-1}\right)$$

for quasimomenta $(K_x, K_y) \in \mathbb{T}^2$ near $(\pi, 0)$ or $(0, \pi)$, where $\alpha > 0$. The Fourier transform $\hat{v}$ is sketched in Fig. 1. α determines the effective mass m^{***} of (dressed) bound fermion pairs, the dispersion relation of which is represented in Fig. 2. Conversely, α can be recovered from m^{***}. An estimate of this mass from

experimental data on La_2CuO_{4+y} can be found in [39]: $m^{***} \in [m_e, 3m_e]$. This parameter has no significant influence on our study because we generally fix the total quansimomentum K. Only the precise shape of Figs. 1 and 2 are dependent on α. Explicit computations explained below demonstrate that $m^{***} \simeq 2m_e$ leads to $\alpha \simeq 1.35$, which is our default value.

THE 2-FERMIONS–1-BIPOLARON SECTOR

Dispersion Relation of Dressed Bound Fermion Pairs

Like in [50], we study the restriction $H^{(2,1)}$ of $\mathbf{H}$ to the invariant space $\mathcal{H}^{(2,1)}_{\uparrow\downarrow}$ of one bipolaron and one fermion pair with zero total spin. By translation invariance, $H^{(2,1)}$ is unitarily equivalent to some decomposable operator

$$A = \frac{1}{(2\pi)^2} \int_{\mathbb{T}^2}^{\oplus} A(K) \, \mathrm{d}^2K \ ,$$

where the fiber Hamiltonians $A(K)$, $K \in \mathbb{T}^2$, are operators acting on the Hilbert space $L^2(\mathbb{T}^2;\mathbb{C}) \times \mathbb{C}$. See Theorem 1. In this representation, the invariant space $\mathcal{H}^{(2,1)}_{\uparrow\downarrow}$ corresponds to

$$\begin{aligned} \mathfrak{F}^{(2,1)}_{\uparrow\downarrow} &\doteq L^2(\mathbb{T}^2; L^2(\mathbb{T}^2;\mathbb{C})) \times L^2(\mathbb{T}^2;\mathbb{C}) \qquad (5) \\ &\equiv \frac{1}{(2\pi)^2} \int_{\mathbb{T}^2}^{\oplus} L^2(\mathbb{T}^2;\mathbb{C}) \oplus \mathbb{C} \, \mathrm{d}^2K \ . \end{aligned}$$

We denote the elements of $\mathfrak{F}^{(2,1)}_{\uparrow\downarrow}$ by (Φ_f, Φ_b), respectively the wave function of one fermion pair and one bipolaron in Fourier space. Bound fermion pairs of *minimum* energy correspond to the low energy solutions of the Schrödinger equation associated with $H^{(2,1)}$. Similar to [50, Lemma 8], the ground state energy E_0, defined as being the infimum of the spectrum of $H^{(2,1)}$, is non-positive. The strict negativity of E_0 corresponds to the formation of a *bound fermion pair*. An explicit criterion for that can be provided. See, e.g., [50, Theorems 2, 3 and discussions thereafter]. We are thus interested in the structure of wave functions in the (invariant) subspace

$$\mathcal{G}_\varepsilon \doteq \mathrm{Ran}\left(\mathbf{1}_{[E_0, E_0(1-\varepsilon)]}(H^{(2,1)}) \right) \ ,$$

for small $\varepsilon > 0$. Here, $\mathbf{1}_{[E_0, E_0(1-\varepsilon)]}(H^{(2,1)})$ is the spectral projection of $H^{(2,1)}$ for the interval $[E_0, E_0\,(1-\varepsilon)]$, while $\mathrm{Ran}(P)$ stands for the range of a projection P. Exactly as done in [50, Sect. 5], the bottom of the spectrum of $H^{(2,1)}$, as well as the space $\mathcal{G}_\varepsilon$, can be determined by studying the ground states of the fiber Hamiltonians $A(K)$, $K \in \mathbb{T}^2$. In particular, the existence of strictly negative eigenvalues $\lambda \equiv \lambda(K, \varkappa\hat{v}(K)) < 0$ of $A(K)$ implies $E_0 < 0$.

One can observe from Fig. 2 that the space $\mathcal{G}_\varepsilon$ of nearly minimal energy ($\varepsilon \ll 1$) is related to those quasimomenta K at which the coupling $|\hat{v}(K)|$ is maximal. That is, $(0,\pi)$ and $(\pi,0)$ in the present case. Therefore, we focus our study on $K = (0,\pi)$, the case $(\pi,0)$ being completely equivalent. Moreover, the same figure gives the dispersion relation of a compound particle, named here *dressed* bound fermion pair, which, at minimum energy, behaves like a *massive* particle. There are two types of such pairs: one which is at rest at total quasimomentum $K = (0,\pi)$; the other one at $K = (\pi,0)$.

By standard perturbation theory for non-degenerate eigenvalues, one computes that, at $K = (0,\pi)$ and $(\pi,0)$,

$$\begin{aligned} &\lambda(K+\eta, \varkappa\hat{v}((K+\eta)) \\ &\quad = \lambda(K,\varkappa) + \partial^2_{K_x}\lambda(K,\varkappa)\frac{\eta_x^2}{2} + \partial^2_{K_y}\lambda(K,\varkappa)\frac{\eta_y^2}{2} \\ &\qquad + \varkappa\partial_\varkappa\lambda(K,\varkappa)\partial^2_{K_x}\hat{v}(K)\frac{|\eta|^2}{2} + \mathcal{O}\left(|\eta|^3\right) \end{aligned}$$

for $\eta \in \mathbb{T}^2$, $|\eta| \ll 1$. Therefore, the mass of the dressed bound fermion pair equals

$$m^{***} = \frac{\mu_{\mathrm{ex}}\mu_0}{\mu_0 + \mu_{\mathrm{ex}}} m_e \in m_e \min\{\mu_{\mathrm{ex}}, \mu_0\}\,[1/2, 1] \ ,$$

where

$$\begin{aligned} \mu_0 &\doteq \frac{\hbar^2}{m_e \mathbf{a}^2} \begin{pmatrix} \frac{1}{\partial^2_{K_x}\lambda(K,\varkappa)} & 0 \\ 0 & \frac{1}{\partial^2_{K_y}\lambda(K,\varkappa)} \end{pmatrix} , \\ \mu_{\mathrm{ex}} &\doteq -\frac{\hbar^2}{2\alpha m_e \mathbf{a}^2 \varkappa \partial_\varkappa \lambda\,(K,\varkappa)} \begin{pmatrix} 1 & 0 \\ 0 & 1 \end{pmatrix} \end{aligned}$$

are respectively the intrinsic and bipolaron-fermion-exchange-induced mass ratios with respect to the electron mass m_e. Recall that $\mathbf{a} = 2.672$Å is the lattice spacing. Numerical estimates at prototypical parameters for $K = (0,\pi)$ yield

$$\mu_0 \simeq \begin{pmatrix} 80 & 0 \\ 0 & -52 \end{pmatrix} \ .$$

For $K = (\pi,0)$, μ_0 is the same, up to a permutation of the diagonal entries. Therefore, to get $m^{***} \simeq 2m_e$ [39], it suffices to have $\mu_{\mathrm{ex}} \simeq 2$, which in turn yields $\alpha \simeq 1.35$, which is our default value. ($m^{***} \in [m_e, 3m_e]$ leads to $\alpha \in [0.9, 2.7]$.)

Being massive particles, dressed bound fermion pairs at total quasimomentum $K = (0,\pi)$ or $K = (\pi,0)$ have a dispersion relation *not* satisfying Landau's criterion of superfluidity [44, p. 318]. Superconductivity in our model is thus expected, as is usual, to be a *collective* phenomenon. This is in accordance with the fact that the binding energy of dressed bound fermion pairs is much larger than the superconducting transition temperature: From Fig. 3 (blue curve), the prototypical coupling strength is $\varkappa \simeq 0.11eV$, leading to a binding energy of about $1250K$ (Fig. 6), much larger than the superconducting transition temperature for La_2CuO_4 at optimal doping, which equals $39K$ [6, Fig. 5.1]. This high binding energy is consistent [74] with the high *pseudogap*

temperature T^* of $La_{1.85}Sr_{0.15}CuO_4$ at optimal doping, which is about $400K$ [32, Fig. 26]. Indeed, by ARPES experiments, at temperatures below T^*, the pseudogap looks crudely like the d–wave superconducting gap. It mainly appears for quasimomenta $(\pi, 0)$ and $(0, \pi)$ in the normalized Brillouin zone. See [2, Fig. 4] and references therein. Quoting [2, p. 4], "This immediately suggests that at the very high pseudogap temperature T^*, pairs already start to form, while phase fluctuations prohibit superconducting order until much lower temperatures are reached." Our model, in the 2-fermions–1-bipolaron sector with prototypical parameters, strongly supports the conjecture of d–wave pair formation in the *pseudogap* regime. This is particularly the case inasmuch as the binding energy of bipolarons goes from about $1500K$ at zero doping to $500K$ at optimal doping [58, Fig. 2], while T^*, in the same doping range, goes from about $750K$ to $400K$ [32, Fig. 26] (and is thus always below $1250K$).

Note that Fig. 6 demonstrates that dressed bound fermion pairs already appear at relatively small exchange coupling strength $\varkappa$, as compared with the hopping amplitude ϵ. Observe also that inter-site repulsions have a large impact on the binding energy, even if their strength is much smaller than that of the on-site repulsion, see Fig. 12. By contrast, a large $U_0 \gg 1$ (hard-core regime) does not change much the binding energy, see Fig. 6. This demonstrates, in the scope of the microscopic theory proposed here, that inter-site repulsions constrain the pseudogap temperature. Note that the idealized situation $r = 0$ (on-site repulsion only) already captures well the physics of the model at prototypical values.

Pairing Modes

The (fiber) space of a fermion pair at constant quasimomentum K is the Hilbert space $L^2(\mathbb{T}^2;\mathbb{C})$ with scalar product

$$\langle\varphi|\psi\rangle \doteq \frac{1}{(2\pi)^2}\int_{\mathbb{T}^2}\overline{\varphi(k)}\psi(k)\ \mathrm{d}^2k.$$

We use the bra-ket notation for elements of this space. They are thus denoted by $|\varphi\rangle$, but the evaluation of the function $|\varphi\rangle$ at fixed $k \in \mathbb{T}^2$ is written as $\varphi(k) \in \mathbb{C}$.

The lattice is invariant under the group $\{0, \pi/2, \pi, 3\pi/2\}$ of rotations, which is generated by the $\pi/2$-rotation. We thus define by

$$[R_\perp|\varphi\rangle]\,(k_x, k_y) \doteq \varphi(k_y, -k_x), \quad (k_x, k_y) \in \mathbb{T}^2,$$

the unitary operator $R_\perp$ implementing the $\pi/2$-rotation on $L^2(\mathbb{T}^2;\mathbb{C})$. Then define the mutually orthogonal projectors

$$P_s \doteq \frac{R_\perp^4 + R_\perp^3 + R_\perp^2 + R_\perp}{4}, \tag{6}$$

$$P_d \doteq \frac{R_\perp^4 - R_\perp^3 + R_\perp^2 - R_\perp}{4}, \tag{7}$$

$$P_p \doteq \frac{R_\perp^4 - R_\perp^2}{2}. \tag{8}$$

Since $P_s + P_d + P_p = \mathbf{1}$, any wave function $|\varphi\rangle \in L^2(\mathbb{T}^2;\mathbb{C})$ of a fermion pair can be uniquely decomposed into orthogonal s-, d- and p-wave components as

$$|\varphi\rangle = |\varphi^s\rangle + |\varphi^d\rangle + |\varphi^p\rangle, \quad |\varphi^\#\rangle \doteq P_\#|\varphi\rangle.$$

Observe that

$$R_\perp|\varphi^s\rangle = |\varphi^s\rangle, \quad R_\perp|\varphi^d\rangle = -|\varphi^d\rangle, \quad R_\perp^2|\varphi^p\rangle = -|\varphi^p\rangle.$$

In particular, if $|\varphi\rangle \in L^2(\mathbb{T}^2;\mathbb{C})$ is invariant with respect to $R_\perp^2$, then $|\varphi^p\rangle$ identically vanishes and $|\varphi\rangle$ has only s- and d-wave components.

Subsequently, we study the eigenvector $(|\psi_K\rangle, 1)$ of $A(K)$ associated with a strictly negative eigenvalue $\lambda \equiv \lambda(K, \varkappa\hat{v}(K)) < 0$ for those total quasimomenta K which maximize the coupling function $|\hat{v}(K)|$, typically $(\pi, 0)$ and $(0, \pi)$. Recall that the exchange coupling strength $\varkappa$ is chosen to get 90% depletion at $(\pi, 0)$ and $(0, \pi)$. The depletion at total quasimomentum K is defined by the ratio

$$\varrho \doteq \frac{100}{(\|\psi_K\|_2^2 + 1)}\% \ .$$

Using prototypical parameters provided in the previous section, Fig. 3 (blue curve) represents this ratio as a function of $\varkappa$ for $K = (0, \pi)$. This leads to $\varkappa \simeq 0.11eV$ when $\varrho \simeq 90\%$.

The dominant (either s-, d- or p-wave) component of $|\psi_K\rangle$ determines the pairing symmetry of the dressed bound fermion pair with total quasimomentum K. By Corollary 1.1, for $K \in \{(0, \pi), (0, \pi)\}$, the p-wave component identically vanishes, that is, $P_p|\psi_K\rangle = 0$. In general [75], ψ_K is a *non-trivial* mixture of s- and d-wave components. Using the prototypical parameters, we derive the s- and d-wave components of the dressed bound fermion pair as a function of $\varkappa$ at $K = (0, \pi)$. See Fig. 4 (blue curves).

For $\varkappa \simeq 0.11eV$, i.e., at 90% depletion, the d-wave pairing is nearly maximized for the prototypical parameters. In this case, one gets

$$\varrho_s \doteq \frac{\|P_s\psi_{(0,\pi)}\|_2^2}{\|\psi_{(0,\pi)}\|_2^2} \times 100\% \simeq 16.5\%$$

s-wave pairing, which is relatively close to the crude estimate (20%-25%) phenomenologically deduced from experimental data [13–15]. See also [8, Section 6].

The (normalized) density $|\check{\psi}_{(0,\pi)}|^2$ of the dressed bound fermion pair in the (relative) position space is represented

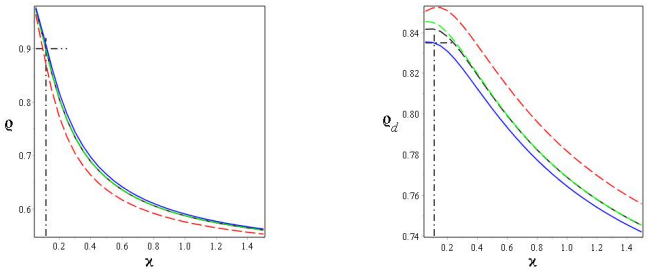

Figure 8: Depletion (left) and d-wave density (right) as functions of $\varkappa$ at total quasimomentum $K = (0, \pi)$ for $r = 0$ (red), 1 (black), 1.5 (green) and 2 (blue).

in Fig. 5. It is anisostropic because of the negative mass in only one of the axes at the van Hove point $(0, \pi)$. The dressed bound fermion pair corresponding to the other van Hove point $(\pi, 0)$ has wave function $|\psi_{(\pi,0)}\rangle = R_{\perp}|\psi_{(0,\pi)}\rangle$. Therefore, up to the $\pi/2$-rotation, it has the same space structure as $|\psi_{(0,\pi)}\rangle$. Both functions are heavily concentrated in a region of *major* diameter $\xi_{\max} \simeq 8$ (in lattice units), i.e., $\xi_{\max} \simeq 8\mathbf{a} = 21.376$Å. This is nearly the same as the coherence length $\xi = 21$Å of $La_{1.8}Sr_{0.2}CuO_4$, which is computed from experimental data via the Ginzburg–Landau theory. See [6, Table 9.1] and references therein. By Fig. 5, the *minor* diameter equals $\xi_{\min} \simeq 6$ (in lattice units), i.e., $\xi_{\min} \simeq 6\mathbf{a} = 16.032$Å. Observe that [39] contributes the estimate $\xi \gtrsim 16$Å for the diameter of the bounded pair, which is derived from experimental data for La_2CuO_{4+y} combined with a simple hydrogenic model (and not from the Ginzburg–Landau theory).

Numerical simulations show that $\xi_{\min}$ and $\xi_{\max}$ do not depend much on the choice of the range r of the repulsion: $\xi_{\max} \simeq 8\mathbf{a}$ and $\xi_{\min} \simeq 6\mathbf{a}$ for all $r = 0, 1, 1.5, 2$. The effects of the parameter r on depletion, d-wave pairing and binding energy, as shown in Figs. 8 and 12 (left), are also minimal. However, changes in r modify the shape of $|\check{\psi}_{(0,\pi)}|^2$. For instance, for $r = 0$ the maximum value of $|\check{\psi}_{(0,\pi)}|^2$ is taken at distance 1 (in lattice units) from the origin, whereas, for $r = 1, 1.5, 2$, its maximum is attained at distance 2. Compare Fig. 5 for $r = 2$ with Fig. 9 for $r = 0$.

As previously explained, the effective mass m^{**} of bipolarons is controversial. Its prototypical value in this study is based on [38]. This corresponds to $h_b \simeq 0.00575$, but in Figs. 10 and 11 we also consider larger values of this parameter, up to the case $h_b = 1$. It turns out that an effective mass m^{**} up to 10 times smaller than the one ($\simeq 695m_e$) estimated in [38] would yield dressed bound fermion pairs with almost exactly the same physical properties as those with default parameters. The (fermion) depletion can never exceed 75% with no dressed bound fermion pairs when $m^{**} \leq 8m_e$ and $\varkappa \leq 0.2eV$, see Figs. 10 and 11. Recall that the effective mass m^* of mobile holes has been measured to be $m^* \simeq 4m_e$

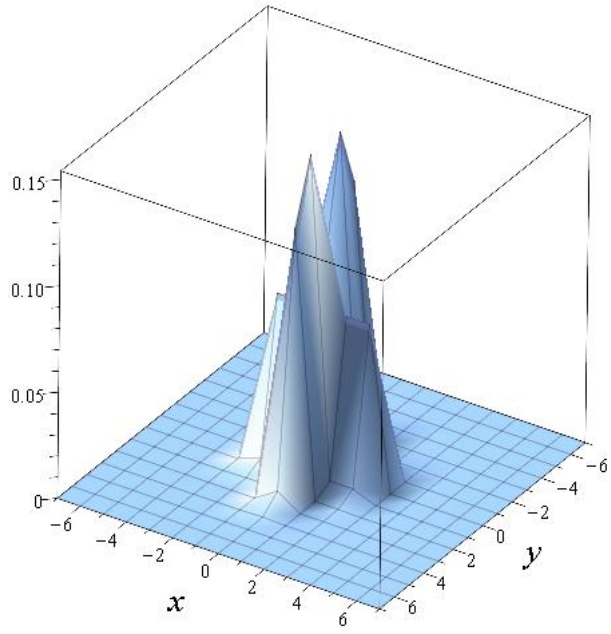

Figure 9: Normalized density $|\check{\psi}_{(0,\pi)}|^2$ of the dressed bound fermion pair as a function of the (relative) position space at total quasimomentum $K = (0, \pi)$ for on-site repulsion ($r = 0$).

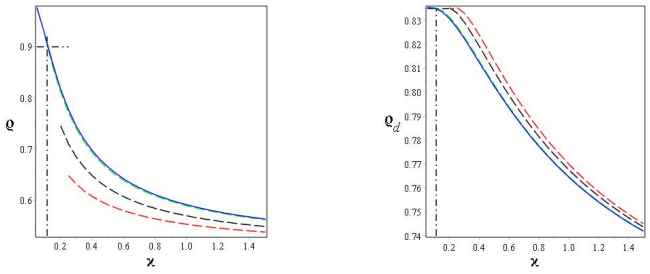

Figure 10: Depletion (left) and d-wave density (right) as functions of $\varkappa$ at total quasimomentum $K = (0, \pi)$ for $h_b = 0.00575$ (blue), 0.0575 (green), 0.575 (black), 1 (red).

[64, Fig. 2.]. Also, the binding energy of dressed bound fermion pairs is strongly reduced for $m^{**} \leq 8m_e$, as compared to the prototypical situation. See Fig. 11. Recall, however, that the small mass computed in [39] is not necessarily in contradiction with the very large mass determined in [38] since, in our model, they refer to the mass of two different quasiparticles: bipolarons in [38] and dressed fermion pairs in [39].

The inter-site nature of bipolarons and the presence of the strong Coulomb repulsion are both essential for a large (> 3) d-wave-to-s-wave ratio. This is seen in Fig. 13, where the blue and red-dashed lines represent the cases $U_0 = U = 0$ (no Coulomb repulsion), and $c_x = 2a_{x,\uparrow}a_{x,\downarrow}$ (on-site bipolarons, not inter-site like in (4)), respectively. Moreover, Fig. 14 demonstrates that the behaviors of the depletion and the pairing are not well-

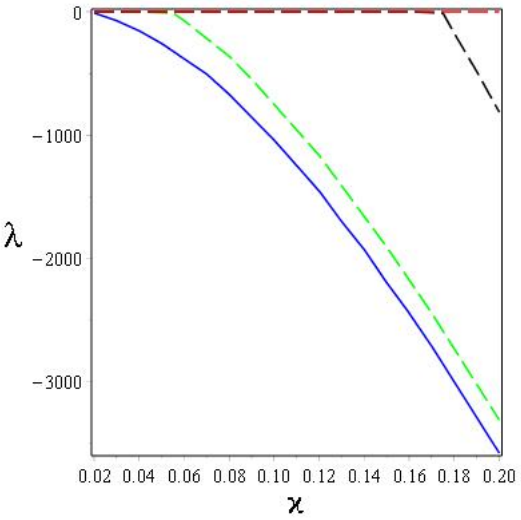

Figure 11: Binding energy λ (in Kelvin) as a function of $\varkappa$ at total quasimomentum $K = (0, \pi)$ for $h_b = 0.00575$ (blue), 0.0575 (green), 0.575 (black), 1 (red).

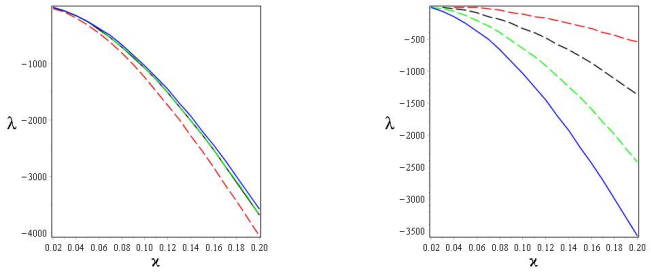

Figure 12: Binding energy λ (in Kelvin) as a function of $\varkappa$ at total quasimomentum $K = (0, \pi)$. In the left figure, $r = 0$ (blue), 1 (green), 1.5 (black), 2 (red). In the right figure, $U = 1.461$ (blue), 5 (green), 15 (black), 50 (red). The vertical and horizontal dot-dashed lines highlight the prototypical parameter $\varkappa = 0.11eV$.

reproduced in the small hopping regime. In particular, the symmetry of dressed fermionic pairs depends not only on the competition between the bipolaron-fermion-exchange interaction and the Coulomb repulsion, but also on the kinetic energy. For instance, in the limit of vanishing hopping (large effective mass of fermions) fermion pairs become purely d-wave with a depletion which does not exceed 75%.

On the other hand, as already discussed, the hard-core regime $U_0 \gg 1$ captures quite well the physical properties of dressed bound fermion pairs, by Figs. 3 (depletion), 4 (s- and d-wave components), and 6 (binding energy). From Fig. 15 note that the strong repulsion regime $U_0 = U \gg \varkappa$ yields a nearly pure d-wave pairing, but is not compatible with 90% depletion. Moreover, the binding energy of dressed bound fermion pairs strongly decreases for large $U_0 = U \gg \varkappa$, by Fig. 12.

We conclude by studying the case where $\hat{v}(K)$ is

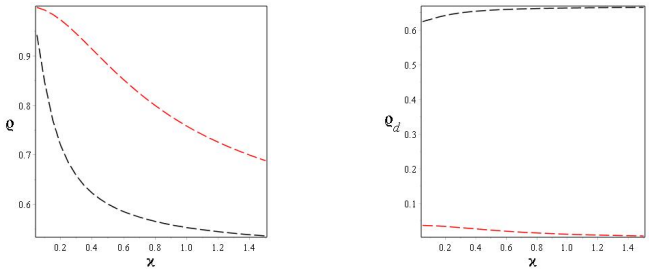

Figure 13: Depletion (left) and d-wave component (right) as functions of $\varkappa$ at total quasimomentum $K = (0, \pi)$ for $U = 0$ (no repulsion, black) and on-site bipolarons (red).

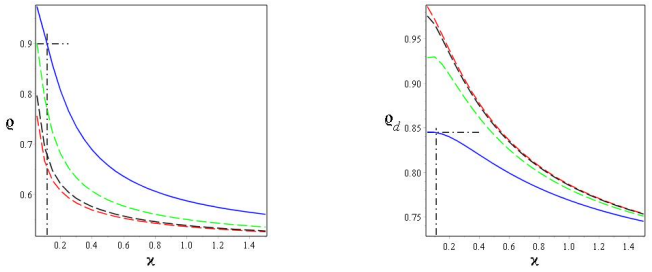

Figure 14: Depletion (left) and d-wave density (right) as functions of $\varkappa$ at total quasimomentum $K = (0, \pi)$ for hopping strengths $\epsilon = 0.266$ (blue), $0.266 \times 25\%$ (green), $0.266 \times 5\%$ (black), $0.266 \times 1\%$ (red). The vertical and horizontal dot-dashed lines highlight the prototypical parameters.

concentrated at $K = (0, \pm\pi/2)$ and $(\pm\pi/2, 0)$, instead of the half-breathing bond-stretching modes $(\pi, 0)$ and $(0, \pi)$. In this case, Corollary 1.1 does not apply anymore and a *non-vanishing* p-wave component of the fermionic wave function appears. At $K = (0, \pi/2)$ (the other cases being equivalent), the s-, d- and p-wave components of $|\psi_{(0,\pi/2)}\rangle$ at prototypical parameters are represented in Fig. 16 as a function of $\varkappa$. We see from this figure that the formation of p-wave pairs is always favored at 90%

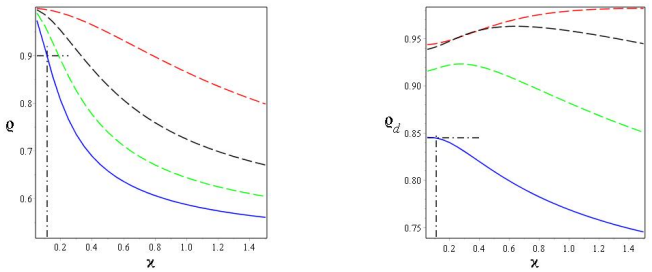

Figure 15: Depletion (left) and d-wave component (right) as functions of $\varkappa$ at total quasimomentum $K = (0, \pi)$ for $U = 1.461$ (blue), 5 (green), 15 (black), 50 (red).

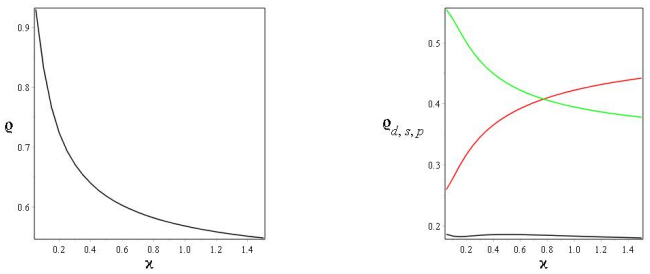

Figure 16: Depletion (left) and s-, d, p-wave densities (right) as functions of $\varkappa$ at total quasimomentum $K = (0, \pi/2)$ for prototypical parameters. The s-, d- and p-wave densities are respectively in red, black and green.

depletion.

This demonstrates that the existence of d-wave pairs in cuprate superconductors is directly related to the fact that $\hat{v}(K)$ is concentrated *near* half-breathing bond-stretching modes ($K = (0, \pi)$, $(\pi, 0)$). Away from those points, p-wave pairs appear and are even dominant at $K = (0, \pm\pi/2)$ and $(\pm\pi/2, 0)$. No p-wave pairs are observed in cuprate superconductors and our study suggests that anomalies near half-breathing bond-stretching modes are therefore part of the physical mechanism leading to the formation of fermion pairs.

Note however that p-wave fermionic pairs has also been observed for non-cuprate high-temperature superconductors. Indeed, the strontium ruthenate Sr_2RuO_4 is at low temperature a superconductor within RuO_2 layers and presents p-wave pairing, see, e.g., [70, Table I]. Nevertheless, our study does not apply to this kind of material because we only consider here spin-singlet fermion pairs; superconducting pairs in Sr_2RuO_4 are spin-triplets, similar to superfluid quantum liquid ^{3}He.

TECHNICAL PROOFS

Preliminaries

The Fourier transform $\hat{v}$ of the rotation symmetric function v, as well as $\epsilon, h_b, \varkappa, U, U_0, r \geq 0$ and $\lambda > 0$, are all fixed. We use here the definition

$$w(z) \doteq U\mathrm{e}^{-\lambda^{-1}|z|} + (U_0 - U)\,\delta_{0,|z|}\,, \quad z \in \mathbb{Z}^2,$$

but the proofs do not depend on this particular choice of w.

Recall that we use the bra-ket notation in $L^2(\mathbb{T}^2;\mathbb{C})$. As usual, $|\varphi\rangle\langle\varphi|$ is seen as an operator on $L^2(\mathbb{T}^2;\mathbb{C})$. In particular, if $|\varphi\rangle$ is normalized, then it is the orthogonal projection on the subspace generated by $|\varphi\rangle$. Similarly, $\langle\varphi|$ is viewed as a map from $L^2(\mathbb{T}^2;\mathbb{C})$ to $\mathbb{C}$.

A special role is played by the normalized vectors $|\mathfrak{e}_z\rangle \in L^2(\mathbb{T}^2;\mathbb{C})$, defined, at all $z \in \mathbb{Z}^2$, by $\mathfrak{e}_z(k) \doteq \mathrm{e}^{-ik\cdot z}$ for $k \in \mathbb{T}^2$. A second family $\{|\mathfrak{f}_K\rangle\}_{K\in\mathbb{T}^2}$ of vectors of $L^2(\mathbb{T}^2;\mathbb{C})$, used below, is defined, for all $K, k \in \mathbb{T}^2$, by

$$\mathfrak{f}_K(k) \doteq 2\,(1 + \cos(K + k) + \cos(K + 2k))) \qquad (9)$$

with $\cos(K) \doteq \cos(K_x) + \cos(K_y)$ for any $K = (K_x, K_y) \in \mathbb{T}^2$.

Fiber Decomposition

Exactly as done in [50, Sect. 5.1], we identify, via the Fourier transform, the space

$$\mathcal{H}^{(2,1)}_{\uparrow\downarrow} \doteq \ell^2(\mathbb{Z}^2 \times \mathbb{Z}^2;\mathbb{C}) \times \ell^2(\mathbb{Z}^2;\mathbb{C})$$

of two fermions and one bipolaron with zero total spin on $\mathbb{Z}^2$ with the Hilbert space $\mathfrak{F}^{(2,1)}_{\uparrow\downarrow}$ (5). The corresponding unitary transformation $\mathfrak{U}$ is the map from $\mathfrak{F}^{(2,1)}_{\uparrow\downarrow}$ to $\mathcal{H}^{(2,1)}_{\uparrow\downarrow}$ defined by $\mathfrak{U}(\Phi_f, \Phi_b) \doteq (\phi_f, \phi_b)$, where

$$\phi_f(x_\uparrow, x_\downarrow) \doteq \frac{1}{(2\pi)^4}\int_{\mathbb{T}^2}\mathrm{d}^2K\int_{\mathbb{T}^2}\mathrm{d}^2k\; \mathrm{e}^{iK\cdot x_\uparrow}\mathrm{e}^{ik\cdot(x_\downarrow - x_\uparrow)}\left[\Phi_f\left(K\right)\right](k)$$

for any $x_\uparrow, x_\downarrow \in \mathbb{Z}^2$ and $\Phi_f \in L^2(\mathbb{T}^2; L^2(\mathbb{T}^2;\mathbb{C}))$, while, for any $x_b \in \mathbb{Z}^2$ and $\Phi_b \in L^2(\mathbb{T}^2;\mathbb{C})$,

$$\phi_b(x_b) \doteq \frac{1}{(2\pi)^2}\int_{\mathbb{T}^2}\mathrm{e}^{iK\cdot x_b}\Phi_b\left(K\right)\mathrm{d}^2K.$$

Similar to [50, Sect. 5.1], we now introduce, for any fixed $K \in \mathbb{T}^2$, five operators as follows:

$A^{(0)}_{1,1}$: We define the bounded self-adjoint operator $A^{(0)}_{1,1}(K)$ acting on $L^2(\mathbb{T}^2;\mathbb{C})$ by

$$[A^{(0)}_{1,1}(K)\varphi](k) \doteq \epsilon(4 - \cos(k - K) - \cos(k))\varphi(k) \quad (10)$$

for any $K, k \in \mathbb{T}^2$. See [50, Eq. (41)].

$A^{(1)}_{1,1}$: Then, for any $K \in \mathbb{T}^2$, the (self-adjoint) operator, which generalizes the one used in [50, Eq. (42)], is defined by

$$A^{(1)}_{1,1}(K) \doteq A^{(0)}_{1,1}(K) + \sum_{z\in\mathbb{Z}^2, |z|\leq r} w(z)|\mathfrak{e}_z\rangle\langle\mathfrak{e}_z|. \quad (11)$$

$A_{2,1}$: Similar to [50, Eq. (43)], for any $K \in \mathbb{T}^2$, the vector $|\mathfrak{f}_K\rangle$ defined by (9) yields the bounded operator $A_{2,1}(K) : L^2(\mathbb{T}^2;\mathbb{C}) \to \mathbb{C}$ defined by

$$A_{2,1}(K) \doteq \hat{v}(K)\langle\mathfrak{f}_K|.$$

$A_{1,2}$: For any $K \in \mathbb{T}^2$, the adjoint of $A_{2,1}(K)$ is the map $A_{1,2}(K)$ from $\mathbb{C}$ to $L^2(\mathbb{T}^2;\mathbb{C})$ defined by

$$A_{1,2}(K)c \doteq c\hat{v}(K)|\mathfrak{f}_K\rangle, \qquad c \in \mathbb{C}. \qquad (12)$$

$A_{2,2}$: For any $K \in \mathbb{T}^2$, $A_{2,2}(K)$ is the map [50, Eq. (45)] from $\mathbb{C}$ to itself defined by

$$A_{2,2}(K)c \doteq \epsilon h_b(2-\cos(K))c, \qquad c \in \mathbb{C}.$$

Now, similar to [50, Sect.5.1, Eq. (46)], the operators

$$A(K) \doteq \begin{pmatrix} A^{(1)}_{1,1}(K) & A_{1,2}(K) \\ A_{2,1}(K) & A_{2,2}(K) \end{pmatrix}, \quad K \in \mathbb{T}^2, \tag{13}$$

acting on the Hilbert space $L^2(\mathbb{T}^2;\mathbb{C})\times\mathbb{C}$, correspond to the fiber decomposition of the operator $\mathfrak{U}^* H^{(2,1)} \mathfrak{U}$:

Theorem 1.

$$A \doteq \mathfrak{U}^* H^{(2,1)} \mathfrak{U} = \frac{1}{(2\pi)^2} \int_{\mathbb{T}^2}^{\oplus} A(K)\, \mathrm{d}^2K.$$

Proof. For any $(\phi_f, \phi_b) \in \mathcal{H}^{(2,1)}_{\uparrow\downarrow}$, one explicitly computes the pair of functions $(\tilde{\phi}_f, \tilde{\phi}_b) \doteq H^{(2,1)}(\phi_f, \phi_b)$:

$$\begin{aligned}\tilde{\phi}_f(x_\uparrow, x_\downarrow) = & \sum_{z\in\mathbb{Z}^2, |z|\leq r} w(z)\, \delta_{x_\uparrow, x_\downarrow + z} \phi_f(x_\uparrow, x_\downarrow) \\ & - \frac{\epsilon}{2} \sum_{z\in\mathbb{Z}^2,|z|=1} \big(\phi_f(x_\uparrow + z, x_\downarrow) + \phi_f(x_\uparrow, x_\downarrow + z)\big) \\ & + 4\epsilon \phi_f(x_\uparrow, x_\downarrow) \\ & + \varkappa \sum_{x_b, z\in\mathbb{Z}^2, |z|\leq 1} v(x_\uparrow - x_b) \left(\delta_{x_\uparrow + z, x_\downarrow} + \delta_{x_\uparrow + z, x_\downarrow - z}\right) \phi_b(x_b)\end{aligned}$$

for all $x_\uparrow, x_\downarrow \in \mathbb{Z}^2$, while the bosonic wave function at $x_b \in \mathbb{Z}^2$ is equal to

$$\begin{aligned}\tilde{\phi}_b(x_b) = & \, 2\epsilon h_b \phi_b(x_b) - \frac{\epsilon h_b}{2} \sum_{z\in\mathbb{Z}^2,|z|=1} \phi_b(x_b + z) \\ & + \varkappa \sum_{x,z\in\mathbb{Z}^2,|z|\leq 1} v(x_b - x) \left(\phi_f(x+z, x) + \phi_f(x+z, x-z)\right) .\end{aligned}$$

Applying the Fourier transformation $\mathfrak{U}^*$ to (ϕ_f, ϕ_b) and $(\tilde{\phi}_f, \tilde{\phi}_b)$, we get the two vectors $(\Phi_f, \Phi_b) \doteq \mathfrak{U}^*(\phi_f, \phi_b)$ and $(\tilde{\Phi}_f, \tilde{\Phi}_b) \doteq \mathfrak{U}^*(\tilde{\phi}_f, \tilde{\phi}_b)$. Using the previous definition of $A(K)$, these vectors are related to each other via the equations

$$\begin{aligned}|\tilde{\Phi}_f(K)\rangle &= A^{(1)}_{1,1}(K)|\Phi_f(K)\rangle + A_{1,2}(K)\Phi_b(K) \\ \tilde{\Phi}_b(K) &= A_{2,1}(K)|\Phi_f(K)\rangle + A_{2,2}(K)\Phi_b(K)\end{aligned}$$

for all $K \in \mathbb{T}^2$. Then the assertion follows, like in [50, Lemma 7]. ∎

Ground States of Fiber Hamiltonians

Exactly as in [50, Lemma 8],

$$E_0 \doteq \min \mathrm{spec}(H^{(2,1)}) = \min_{K\in\mathbb{T}^2} \{\min \mathrm{spec}(A(K))\} .$$

To examine the spectrum of $A(K)$, $K \in \mathbb{T}^2$, we proceed in the same way as in [50, Sect. 5.2], using the Birman-Schwinger principle [50, Proposition 26]: For all $\epsilon, h_b \geq 0$ and $K \in \mathbb{T}^2$, $\lambda < 0$ is an eigenvalue of $A(K)$ iff it solves the equation

$$|\hat{v}(K)|^2 \langle \mathfrak{f}_K | (A^{(1)}_{1,1}(K) - \lambda)^{-1} \mathfrak{f}_K \rangle = \epsilon h_b(2-\cos(K)) - \lambda. \tag{14}$$

Moreover, if the strictly negative eigenvalue exists, the bosonic component of the corresponding eigenvector is non-vanishing. Compare with [50, Lemma 9, Eq. (53)].

For any fixed $K \in \mathbb{T}^2$, it is therefore important to derive a more explicit representation for the left-hand side of (14), like in [50, Lemma 14]. The computation of this scalar product involves the inverse of a finite dimensional matrix whose entries are integrals on the two-dimensional torus $\mathbb{T}^2$ of explicit functions. This inverse is then *numerically* determined.

To explain this, for all $r \geq 0$, define the finite (index) set

$$I^{(r)} \doteq \{z \in \mathbb{Z}^2 : |z| \leq r\} \cup \{\mathfrak{f}\}.$$

Next, for any $j \in \{0,1\}$, define the self-adjoint $I^{(r)} \times I^{(r)}$ matrix $\mathfrak{R}^{(j)}$ by

$$\begin{aligned}\mathfrak{R}^{(j)}_{\mathfrak{f},\mathfrak{f}} &\doteq \langle \mathfrak{f}_K | (A^{(j)}_{1,1}(K) - \lambda \mathbf{1})^{-1} \mathfrak{f}_K \rangle, \\ \mathfrak{R}^{(j)}_{z,\mathfrak{f}} &\doteq \langle \mathfrak{e}_z | (A^{(j)}_{1,1}(K) - \lambda \mathbf{1})^{-1} \mathfrak{f}_K \rangle \doteq \overline{\mathfrak{R}^{(j)}_{\mathfrak{f},z}}, \\ \mathfrak{R}^{(j)}_{z,\tilde{z}} &\doteq \langle \mathfrak{e}_z | (A^{(j)}_{1,1}(K) - \lambda \mathbf{1})^{-1} \mathfrak{e}_{\tilde{z}} \rangle,\end{aligned}$$

for any $z, \tilde{z} \in I^{(r)} \cap \mathbb{Z}^2$. Additionally, we define the $I^{(r)} \times I^{(r)}$ matrix $\tilde{\mathfrak{R}}^{(0)}$ by

$$\tilde{\mathfrak{R}}^{(0)}_{i,\mathfrak{f}} \doteq 0 \qquad \text{and} \qquad \tilde{\mathfrak{R}}^{(0)}_{i,z} \doteq w(z) \mathfrak{R}^{(0)}_{i,z} \tag{15}$$

for all $i \in I^{(r)}$ and $z \in I^{(r)} \cap \mathbb{Z}^2$.

By (10), $\mathfrak{R}^{(0)}$ and $\tilde{\mathfrak{R}}^{(0)}$ are finite dimensional matrices whose entries are integrals on $\mathbb{T}^2$ of *explicit* trigonometric functions. For instance,

$$\mathfrak{R}^{(0)}_{\mathfrak{f},\mathfrak{f}} = \int_{\mathbb{T}^2} \frac{(2\pi)^{-2} |\mathfrak{f}_K(k)|^2}{\epsilon(4 - \cos(k-K) - \cos(k)) - \lambda}\, \mathrm{d}^2k.$$

Then, one gets the following assertion:

Lemma 1. *For any fixed $K \in \mathbb{T}^2$, the $I^{(r)} \times I^{(r)}$ matrices $\mathfrak{R}^{(1)}$, $\mathfrak{R}^{(0)}$ and $\tilde{\mathfrak{R}}^{(0)}$ are related to each other by the equation*

$$\mathfrak{R}^{(0)} = (\mathbf{1} + \tilde{\mathfrak{R}}^{(0)}) \mathfrak{R}^{(1)} .$$

Proof. We infer from (11) and the resolvent equation that

$$\begin{aligned}&(A^{(0)}_{1,1}(K) - \lambda\mathbf{1})^{-1} (A^{(1)}_{1,1}(K) - \lambda\mathbf{1}) \\ &= \mathbf{1} + (A^{(0)}_{1,1}(K) - \lambda\mathbf{1})^{-1} \sum_{z\in\mathbb{Z}^2, |z|\leq r} w(z) |\mathfrak{e}_z\rangle\langle\mathfrak{e}_z|\end{aligned} \tag{16}$$

for any fixed $K \in \mathbb{T}^2$. This equation directly yields the equality

$$\mathfrak{R}^{(0)}_{i,j} = \mathfrak{R}^{(1)}_{i,j} + \sum_{z\in\mathbb{Z}^2,|z|\leq r} w(z)\mathfrak{R}^{(0)}_{i,z}\mathfrak{R}^{(1)}_{z,j}$$

for all $i, j \in I^{(r)}$, which in turn yields the assertion. ■

By numerical methods one can explicitly check that -1 is not an eigenvalue of $\tilde{\mathfrak{R}}^{(0)}$ and, in that case, this lemma uniquely determines $\mathfrak{R}^{(1)}$ from the explicit matrices $\tilde{\mathfrak{R}}^{(0)}$ and $\mathfrak{R}^{(0)}$. Using this observation and (14), the eigenvalue $\lambda \equiv \lambda(K, \varkappa\hat{v}(K))$ of $A(K)$ can be numerically computed, at any fixed $K \in \mathbb{T}^2$.

We look for strictly negative eigenvalues $\lambda < 0$ to get a (dressed) bound fermion pair in the ground state. We restrict our study, without loss of generality, to eigenvectors of the form $(|\psi_K\rangle, 1)$, whose fermionic part can be *explicitly* given in terms of the numbers $\{\mathfrak{R}^{(1)}_{z,\mathfrak{f}}\}_{|z|\leq r}$:

Lemma 2. *For any fixed $K \in \mathbb{T}^2$ and eigenvalue $\lambda < 0$ of $A(K)$,*

$$|\psi_K\rangle = \hat{v}(K)(A^{(0)}_{1,1}(K) - \lambda\mathbf{1})^{-1}\left(\sum_{|z|\leq r} w(z)\mathfrak{R}^{(1)}_{z,\mathfrak{f}}|\mathfrak{e}_z\rangle - |\mathfrak{f}_K\rangle\right)$$

Proof. The proof is a direct consequence of Eqs. (10), (12), (13) and (16) together with the fact that $A(K)(|\psi_K\rangle, 1) = \lambda(|\psi_K\rangle, 1)$. ■

Since, by (10), $A^{(0)}_{1,1}(K)$ is a multiplication operator, one gets from this lemma an explicit expression of the fermionic part $|\psi_K\rangle$ of the eigenvector of $A(K)$ associated with a strictly negative eigenvalue $\lambda < 0$. By (6)-(8), the s-, d- and p-wave components of $|\psi_K\rangle$ can then be numerically determined for any $K \in \mathbb{T}^2$.

For half-breathing bond-stretching modes one concludes from Lemma 2 that the p-wave component is automatically zero:

Corollary 1.1. *Let $|\psi_K\rangle$ be the fermionic part of the eigenvector of $A(K)$ associated with a strictly negative eigenvalue $\lambda < 0$. Then, for $K \in \{(0,\pi),(0,\pi)\}$, $P_p|\psi_K\rangle = 0$, where P_p is the projection defined by (8).*

Proof. If $K \in \{(0,\pi),(0,\pi)\}$ then we infer from (9) that $\mathfrak{f}_K(-k) = \mathfrak{f}_K(k)$, while, by (10)-(11), the operators $A^{(0)}_{1,1}(K)$ and $A^{(1)}_{1,1}(K)$ preserve this symmetry. Therefore, $\mathfrak{R}^{(1)}_{z,\mathfrak{f}} = \mathfrak{R}^{(1)}_{-z,\mathfrak{f}}$ for any $z \in \mathbb{Z}^2$, and we deduce from Lemma 2 that $|\psi_K\rangle$ is invariant under reflection over the origin. The assertion then follows. Note that we use here the reflection symmetry of the interaction kernels w. ■

Acknowledgements. This research is supported by the FAPESP under Grant 2016/02503-8, CNPq, as well as by the Basque Government through the grant IT641-13 and the BERC 2014-2017 program, and by the Spanish Ministry of Economy and Competitiveness MINECO: BCAM Severo Ochoa accreditation SEV-2013-0323, MTM2014-53850.

* Electronic address: jb.bru@ikerbasque.org
† Electronic address: wpedra@if.usp.br
‡ Electronic address: amsiddp@if.usp.br

[1] M. Imada, A. Fujimori, and Y. Tokura, Metal-insulator transitions, Rev. Mod. Phys. **70** (1998) 1039–1263
[2] B. Keimer *et al.*, From quantum matter to high-temperature superconductivity in copper oxides, Nature **518** (2015) 179–186
[3] K.A. Müller, J.G. Bednorz, Possible high T_c superconductivity in the Ba-La-Cu-O system, Z. Phys. B. **64**(2) (1986) 189–193
[4] A.K. Saxena, High-Temperature Superconductors, Springer-Verlag, Berlin Heidelberg (2010)
[5] N. Plakida, High-Temperature Cuprate Superconductors, Experiment, Theory, and Applications, Springer-Verlag, Berlin Heidelberg (2010)
[6] R. Wesche, Physical Properties of High-Temperature Superconductors, Wiley series in materials for electronic and optoelectronic applications (2015)
[7] C.C. Tsuei and J.R. Kirtley, Pairing symmetry in cuprate superconductors, Rev. Mod. Phys. **72**(4) (2000) 969–1016
[8] K.A. Müller, On the superconductivity in hole doped cuprates, J. Phys.: Condens. Matter, **19** (2007) 251002 (13pp)
[9] H. Keller, A. Bussmann–Holder, K.A. Müller, Jahn–Teller physics and high–T_c superconductivity, Materials Today **11**(9) (2008) 38–46
[10] K.A. Müller, On the macroscopic s- and d-wave symmetry in cuprate superconductors, Phil. Mag. Lett. **82**(5) (2002) 279–288
[11] K.A. Müller, On the symmetry of the superconducting wavefunction in the cuprates, in Applied Superconductivity 2003, edited by A. Andreone *et al*, Ins. Phys. Conf. Series **181** (2003) 3–10
[12] Z. Y. Liu *et al*, Bulk evidence for s-wave pairing symmetry in electron-doped infinite-layer cuprate $Sr_{0.9}La_{0.1}CuO_2$, Europhys. Lett. **69**(2) (2005) 263–269
[13] K.A. Müller and H. Keller, High-Tc Superconductivity 1996: Ten Years After the Discovery, NATO ASI Ser. E **343** (1996) Dordrecht: Kluwer
[14] R. Kasanov *et al*, Experimental Evidence for Two Gaps in the High-Temperature $La_{1.83}Sr_{0.17}CuO_4$ Superconductor, Phys. Rev. Lett. **98** (2007) 057007 (4pp)
[15] A. Furrer, Admixture of an s-Wave Component to the d-Wave Gap Symmetry in High-Temperature Superconductors, J. Supercond. Nov. Magn. **21** (2008) 1–5
[16] A. Bussmann-Holder *et al*, Polaron Coherence as Origin of the Pseudogap Phase in High Temperature Superconducting Cuprates, J. Supercond. Nov. Magn. **21** (2008) 353–357
[17] L. Liu *et al*, Phases of the infinite U Hubbard model on square lattices, Phys. Rev. Lett. **108** (2012) 126406 (4pp)
[18] N. Datta, R. Fernández, and J. Fröhlich, Effective Hamiltonians and phase diagrams for tight-binding models, Journal of Statistical Physics **96**(3) (1999) 545–611
[19] G.M. Zhao and A.S. Alexandrov, Consistent explana-

tions of tunneling and photoemission data in cuprate superconductors: No evidence for magnetic pairing, cond-mat/arXiv:1208.3128v2 (2012)
[20] H. Köppel, D.R. Yarkony and H. Barentzen, The Jahn-Teller Effect: Fundamentals and Implications for Physics and Chemistry, Springer (2009)
[21] A.M. Stoneham and L.W. Smith, Defect phenomena in superconducting oxides and analogous ceramic oxides, J. Phys.: Condens. Matter **3** (1990) 225–278
[22] A.S. Alexandrov and G.M. Zhao, Isotope effects in high-T_c cuprate superconductors as support for the bipolaron theory of superconductivity, New Journal of Physics **14** (2012) 013046 (10pp)
[23] Y. Maeno *et al.*, Superconductivity in a layered perovskite without copper, Nature **372** (1994) 532–534
[24] A.P. Mackenzie and Y. Maeno, The superconductivity of $Sr_2RuO_4$and the physics of spin-triplet pairing, Rev. Mod. Phys. **75**(2) (2003) 657–712
[25] J.P. Hague, P.E. Kornilovitch, J.H. Samson, and A.S. Alexandrov, Superlight Small Bipolarons in the Presence of a Strong Coulomb Repulsion, Phys. Rev. Lett. **98** (2007) 037002 (4pp)
[26] A.S. Alexandrov, Bose–Einstein condensation of strongly correlated electrons and phonons in cuprate superconductors, J. Phys.: Condens. Matter **19** (2007) 125216 (23pp)
[27] A.S. Alexandrov, Theory of high-temperature superconductivity in doped polar insulators, EPL **95** (2011) 27004 (5pp)
[28] A.S. Alexandrov, High-temperature superconductivity: the explanation, Phys. Scr. **83** (2011) 038301 (8pp)
[29] A.S. Alexandrov, Theory of high temperature superconductivity beyond BCS with realistic Coulomb and Fröhlich interactions, J. Supercond. Nov. Magn. **26**(4) (2013) 1313–1317
[30] A. Bussmann-Holder and H. Keller, Polaron formation as origin of unconventional isotope effects in cuprate superconductors, Eur. Phys. J. B **44** (2005) 487–490
[31] P. Rodgers, Superconductivity debate gets ugly, Physics World (1998).
[32] T. Timusk and B. Statt, The pseudogap in high-temperature superconductors: an experimental survey, Rep. Prog. Phys. **62** (1999) 61–122
[33] J. Ranninger and S. Robaszkiewicz, Superconductivity of locally paired electrons, Phys. B **135** (1985) 468–472
[34] J. Ranninger, The polaron scenario for high-T_c superconductivity, Phys. C: Superconductivity and its applications **235** (1994) 277–280
[35] J. Ranninger and J.M. Robin, The boson-fermion model of high-Tc superconductivity Doping dependence, Phys. C **253** (1995) 279–291
[36] S.P. Ionov, Izv. Akad. Nauk, **49** (1985) 310 ; English translation: Bull. Acad. Sci. USSR, Phys. Ser. (USA) A **49** (1985) 90
[37] K.H. Höck, H. Nickisch and H. Thomas, Jahn-Teller Effect in Itinerant Electron Systems: The Jahn-Teller Polaron, Helv. Phys. Acta **56** (1983) 237–243
[38] D. Reagor, Large Dielectric Constants and Massive Carriers in La_2CuO_4, Phys. Rev. Lett. **62**(17) (1989) 2048–2051
[39] C.Y. Chen *et al.*, Frequency and magnetic-field dependence of the dielectric constant and conductivity of La_2CuO_{4+y}, Phys. Rev. B **43**(1) (1991) 392–401
[40] D. Mihailovic and K.A. Müller, High-Tc Superconductivity 1996: Ten Years after the Discovery, NATO ASI Ser 343
[41] D. Mihailovic, Optical Experimental Evidence for a Universal Length Scale for the Dynamic Charge Inhomogeneity of Cuprate Superconductors, Phys. Rev. Lett. **94** (2005) 207001 (4pp)
[42] M.P.M. Dean *et al.,* Persistence of magnetic excitations in $La_{2-x}Sr_xCuO_4$ from the undoped insulator to the heavily overdoped non-superconducting metal, Nature Materials **12** (2013) 1019–1023
[43] M. Le Tacon *et al.,* Intense paramagnon excitations in a large family of high-temperature superconductors, Nature Phys. **7** (2011) 725–730
[44] V.A. Zagrebnov and J.-B. Bru, The Bogoliubov Model of Weakly Imperfect Bose Gas, Phys. Rep. **350** (2001) 291–434
[45] J.-B. Bru, Beyond the dilute Bose gas, Phys. A **359** (2006) 306–344
[46] V.B. Geshkenbein, L.B. Ioffe, A.I. Larkin, Superconductivity in a system with preformed pairs, Phys. Rev. B **55**(5) (1997) 3173–3180
[47] V.V. Kabanov and D. Mihailovic, Finite-Wave-Vector Phonon Coupling to Degenerate Electronic States in $La_{2-x}Ba_xCuO_4$, J. Supercond. **13** (2000) 959–962
[48] D. Mihailovic D and V.V. Kabanov, Finite wave vector Jahn-Teller pairing and superconductivity in the cuprates, Phys. Rev. B **63** (2001) 054505 (8pp)
[49] R.J. McQueeney *et al*, Anomalous Dispersion of LO Phonons in $La_{1.85}Sr_{0.15}CuO_4$ at Low Temperatures, Phys. Rev. Lett. **82**(3) (2005) 628–631
[50] J.-B. Bru, W. de Siqueira Pedra, A. Delgado de Pasquale, d-Wave pairing driven by bipolaric modes related to giant electron-phonon anomalies in high-T_c superconductors, J. Stat. Mech. **2015** (2015) P03002 (36pp)
[51] D. Reznik, Giant Electron–Phonon Anomaly in Doped La_2CuO_4 and Others Cuprates, Advances in Condensed Matter Physics **2010** (2010) 523549 (24pp)
[52] P. Aynajian, Electron–Phonon Interaction in Conventional and Unconventional Superconductors, Springer (2010)
[53] L. Pintschovius and W. Reichardt, Phonon dispersions and phonon density-of-states in copper-oxide superconductors, in Neutron Scattering in Layered Copper-Oxide Superconductors, A. Furrer, Ed., vol. 20 of Physics and Chemistry of Materials with Low-Dimensional Structures, pp. 165–223, Kluwer Academic Publishers, Dordrecht, The Netherlands, 1998.
[54] L. Pintschovius, D. Reznik, and K. Yamada, Oxygen phonon branches in overdoped $La_{1.7}Sr_{0.3}CuO_4$. Phys. Rev. B **74** (2006) 174514 (5pp)
[55] D. Reznik *et al.*, Electron-phonon anomaly related to charge stripes: static stripe phase versus optimally doped superconducting $La_{1.85}Sr_{0.15}CuO_4$, J. Low Temp. Phys. **147**(3-4) (2007) 353–364
[56] D. Reznik *et al*, Photoemission kinks and phonons in cuprates, Nature **455**(7213) (2008) E6–E7
[57] J. Noffsinger, F. Giustino, S.G. Louie, and M.L. Cohen, First principles study of superconductivity and Fermi-surface nesting in ultrahard transition metal carbides, Phys. Rev. B **77**(18) (2008) 180507(R) (4pp)
[58] K.A. Müller, G.M. Zhao, K. Conder and H. Keller, The ratio of small polarons to free carriers in $La_{2-x}Ba_xCuO_4$ derived from susceptibility measurements, J. Phys.: Condens. Matter **10** (1998) L291–L296
[59] J.B. Bru and W. de Siqueira Pedra, Effect of a locally repulsive interaction on s–wave superconductors, Rev. Math. Phys. **22**(3) (2010) 233–303
[60] J.B. Bru, W. de Siqueira Pedra, A. Dömel, A microscopic

two–band model for the electron-hole asymmetry in high-$T_c$superconductors and reentering behavior, J. Math. Phys. **52** (2011) 073301 (28pp)

[61] I. Božović, X. He, J. Wu, and A.T. Bollinger, Dependence of the critical temperature in overdoped copper oxides on superfluid density, Nature **536** (2016) 309–311

[62] B.J. Ramshaw *et al.,* Broken rotational symmetry on the Fermi surface of a high-$T_c$superconductor, Quantum Materials **2**(8) (2017) 1–6

[63] B.I. Kochelaev *et al.*, Three-Spin-Polarons and Their Elastic Interaction in Cuprates, Mod. Phys. Lett. B **17**(10, 11 & 12) (2003) 415–421

[64] W.J. Padilla *et al*, Constant effective mass across the phase diagram of high-$T_c$cuprates, Phys. Rev. B **72** (2005) 060511(R) (4pp)

[65] W. Chaibi *et al*, Effect of a magnetic field in photodetachment microscopy, Eur. Phys. J. D **58** (2010) 29–37

[66] J. Mannhart and H. Hilgenkamp, Interfaces involving complex superconductors, Phys. C **317** (1999) 383–391

[67] G.F. Giuliani and G. Vignale, Quantum Theory of the Electron Liquid, Cambrigde Univ. Press (2005)

[68] M.A. Kastner, R.J. Birgeneau, G. Shirane, Y. Endoh, Magnetic transport and optical properties of monolayer copper oxides, Rev. Mod. Phys. **70**(3) (1998) 897–928

[69] E.H. Lieb, N. Rougerie, J. Yngvason, Local incompressibility estimates for the laughlin phase, arXiv:1701.09064 (2017)

[70] Y. Marnoe *et al.*, Evaluation of Spin-Triplet Superconductivity in Sr_2RuO_4, J. Phys. Soc. Jpn. **81** (2012) 011009 (29pp)

[71] Considering a chain of CuO_2 the presence of a JT polaron implies a string of reversed Cu spins behind it.

[72] This means that the fermionic component of the dressed bound fermion pairs becomes very small in comparison with the bipolaronic component.

[73] This corresponds to a lattice spacing of the copper ions equal to 3.779Å.

[74] For instance, the standard enthalpy of formation of Carbon monoxide is $-110.5kJmol^{-1}$, corresponding to $13290K$, whereas the thermal decomposition of this gas is about $4200K$ (the highest known decomposition temperature). For water (as a gas), the standard enthalpy of formation is $-241.818kJmol^{-1}$, corresponding to $29084K$, with a thermal decomposition of about $2300K$.

[75] For $\varkappa = 1$, $r = 0$, $K \in \{(0,\pi),(0,\pi)\}$, the s-wave component only vanishes in the limit $\epsilon \to 0$, $U \to \infty$, by [50, Theorem 4].